Channel Equalization for Self-Synchronizing Chaotic Systems

by

Richard J. Barron

B.S., University of Illinois at Urbana-Champaign (1994)

Submitted to the
Department of Electrical Engineering and Computer Science
in partial fulfillment of the requirements for the degree of

Master of Science

at the

MASSACHUSETTS INSTITUTE OF TECHNOLOGY

June 1996

© Massachusetts Institute of Technology 1996. All rights reserved.

Author ____________________
Department of Electrical Engineering and Computer Science
May 13, 1996

Certified by ____________________
Alan V. Oppenheim
Distinguished Professor of Electrical Engineering
Thesis Supervisor

Accepted by ____________________
Frederic R. Morgenthaler
Chairman, Departmental Committee on Graduate Students

MASSACHUSETTS INSTITUTE
OF TECHNOLOGY

JUL 16 1996

LIBRARIES

Eng.

Channel Equalization for Self-Synchronizing Chaotic Systems

by

Richard J. Barron

Submitted to the Department of Electrical Engineering and Computer Science
on May 13, 1996, in partial fulfillment of the
requirements for the degree of
Master of Science

Abstract

Many areas of science and engineering have explored and utilized the chaotic behavior of certain nonlinear dynamical systems. Potentially useful communications schemes have been proposed that exploit the broadband, noise-like properties of chaotic signals. Most strategies proposed for utilizing chaotic signals for communications exploit the self-synchronization property of a class of chaotic systems. Typical transmission channels introduce distortion including time-varying attenuation due to fading, scattering, etc., and modification of the spectral characteristics due to channel filtering and multipath effects that significantly degrade synchronization of the chaotic transmitter and receiver. The focus of this thesis is on equalization of these channel effects to restore synchronization. Estimation and compensation for the channel distortions are achieved through the use of the properties of the transmitted chaotic signals and the synchronization property of the receiver.

Thesis Supervisor: Alan V. Oppenheim
Title: Distinguished Professor of Electrical Engineering

Acknowledgments

I would like to thank my advisor, Alan V. Oppenheim, for always seeing the best in me, and pushing me to be better. I value his insight and wisdom which have straightened me out on many occasions.

I thank Kevin Cuomo for sharing with me his vast knowledge of chaos in our many technical discussions.

I thank the members of the M.I.T. Digital Signal Processing Group. Many of our informal technical discussions have inspired valuable ideas. DSPG members have also provided me with an escape from the rigors of research when I have needed it most.

Contents

1 Introduction **11**

1.1 Definitions and Motivations 11

1.2 Self-Synchronization in Chaotic Systems 13

1.3 Self-synchronization and the Lorenz System 15

1.4 Outline of Thesis 17

2 Digital Implementation of Self-Synchronizing Transmitter-Receiver Pair **19**

2.1 Numerical Integration of Dynamic Equations 19

2.1.1 Uniform Integration Step Size 20

2.1.2 Composite Implementation 20

2.1.3 Independent Transmitter-Receiver Implementation 21

2.2 Numerical Experiments 23

2.3 Conclusion 25

3 Equalization for Channel Gain **27**

3.1 Average Power Normalization 27

3.2 Adaptive Error Minimization 31

3.3 Effect of Linearly Varying Gain on Average Power Equalization . . . 33

3.4 Effect of Linearly Varying Gain on Adaptive Error Minimization Equalization 33

3.5 Numerical Experiments: Comparison of Average Power Normalization and Adaptive Error Minimization 36

3.6 Conclusion 38

4 Equalization of Minimum Phase Channels 39

4.1 Introduction 39

4.2 Power Spectral Division 40

4.3 Minimum Phase Filter Response from Band-limited Magnitude 41

4.4 Numerical Experiments 43

4.5 Conclusion 46

5 Equalization of Linear Time Invariant Channels 49

5.1 Introduction 49

5.2 The Error Power Surface 50

5.3 Steepest Descent Implementation 50

5.4 Starting Point for the Steepest Descent Iteration: Initial Equalizer Estimate 52

5.5 Exhaustive Search of Initial Equalizer Zero Placements 53

5.6 Steepest Descent with Respect to Allpass Poles 54

5.7 Numerical Experiments 56

5.8 Conclusion 59

6 System Identification Using Self-Synchronizing Chaotic Signals 61

6.1 Introduction 61

6.2 Numerical Experiment 62

7 Summary and Contributions 65

7.1 Channel Gain Equalization 65

7.2 Equalization of Minimum Phase Channels 66

7.3 Equalization of Linear Time-Invariant Channels 67

7.4 System Identification Using Self-Synchronizing Chaotic Signals 69

A Approximate Analysis of the Effect of Linearly Varying Channel Gain on an Average Power Estimate 71

A.1 Case 1: Power Estimate for Constant Gain 72
A.2 Case 2: Power Estimate for Linearly Varying Gain 72

List of Figures

1-1 The Lorenz Attractor 12

1-2 Communications with Self-Synchronizing Chaotic signals 13

1-3 a) Lorenz drive signal and synchronizing receiver signal. b) Error signal 16

2-1 Impulse response and frequency response of zero-order hold 23

2-2 Synchronization error vs. time using zero-order hold ($\Delta = .0025, .005$) and band-limited interpolation ($\Delta = .005$) on the receiver input . . . 24

3-1 Synchronization error vs. time for $G(t) = 2$ and no compensation . . 29

3-2 Block diagram of gain compensation strategy 29

3-3 $G(t)Q(t)$ using a 5 second window for $x_r(t) = 2x(t)$, where x(t) is a Lorenz drive signal 30

3-4 Synchronization error power vs constant gain, G 31

3-5 (a) Time varying gain $G(t) = 1 - (t - 10)/20$, (b) Corresponding synchronization error versus time, (c) Minimum error Gain $Q_{me}(10)Q(10)G(t)$, (d) Error corresponding to gain in (c) 35

3-6 Synchronization error reduction after equalization of constant gain channel. $G(t) = 2$. 37

3-7 Synchronization error after equalization of time varying gain channel. $G(t) = 1 + t/10$. 37

4-1 Power spectrum of Lorenz signal 40

4-2 Power spectra of Butterworth channel and scaled Lorenz signal 44

4-3 Actual and Estimated magnitude of Butterworth channel 45

4-4 Error versus time for Butterworth channel. a) without compensation, b) with compensation 46

5-1 Steepest Descent Implementation for an FIR equalizer 50
5-2 Steepest Descent Implementation for Minimum Phase/Allpass equalizer 54
5-3 Channel Response 56
5-4 Response of channel in cascade with all-pole modeling equalizer (-) and error minimization equalizer (- -) 57
5-5 - - Error for all-pole modeling equalizer, - Error for steepest descent equalizer 58

6-1 a) Channel magnitude response (-), stochastic estimate (-.), and Lorenz estimate (- -). b) Phase response 63

Chapter 1

Introduction

1.1 Definitions and Motivations

Many areas of science and engineering have explored and utilized the chaotic behavior of certain nonlinear dynamical systems. Although no definition is universally accepted, an appropriate definition of chaos involves three main characteristics. Chaos is *aperiodic, long-term* behavior occurring in a *deterministic system* that exhibits *sensitive dependence on initial conditions* [1]. Sensitive dependence on initial conditions means that if there exists any error in an initial state estimate, the error between the actual state and the state estimate grows exponentially with time. This property translates to the noise-like characteristic of poor longterm predictability. The aperiodicity of chaotic signals results in a broadband power spectrum that lacks the discrete frequency peaks of periodic or quasiperiodic signals. The fact that chaotic waveforms are generated from a deterministic system, in conjunction with the noise-like properties of these signals, suggests potential for the use of synthesized chaotic signals in engineering.

Figure 1-1 shows the evolution in 3 dimensional phase space of the Lorenz system of equations operating in a chaotic regime. The specific equations for the Lorenz system are given in Section 1.3. As is apparent from the figure, the trajectory is confined to a limiting space, or attractor. The Lorenz system is an example of a dissipative chaotic system. A dissipative chaotic system is one whose limiting trajectories

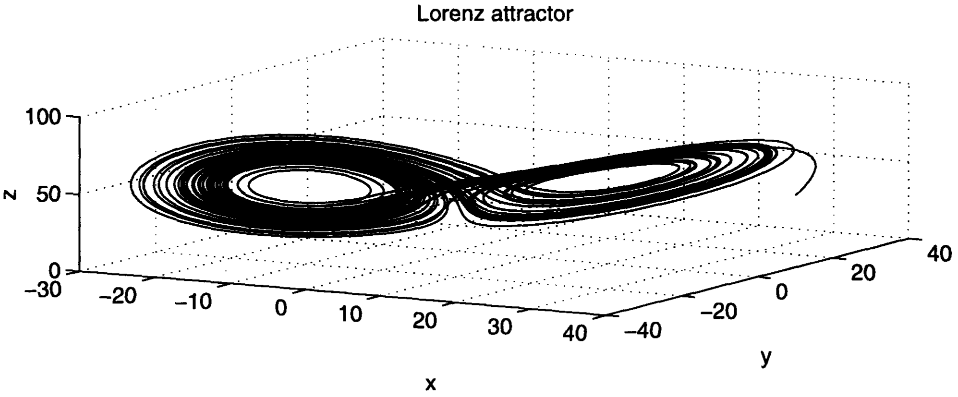

Figure 1-1: The Lorenz Attractor

occupy a region in state space of zero volume and fractional dimension. Although locally unstable, trajectories on this limiting set are bounded in a region of state space.

There exists a certain class of dissipative chaotic systems that are *self-synchronizing*, which is of significant practical interest. Two chaotic systems synchronize, i.e. they follow the same trajectories, by sharing a chaotic reference signal, or drive signal. For such pairs, synchronization occurs regardless of the initial conditions of either system.

By making the two systems part of a transmitter-receiver pair, potentially useful communications schemes have been proposed that exploit the broadband, noise-like properties of the chaotic signals. The transmitted drive signal can be used as a mask for information bearing waveforms or as a modulating signal in spread-spectrum systems [2, 3].

In any proposed communication scheme utilizing self-synchronizing chaotic systems, it is imperative to maintain synchronization between transmitter and receiver. Typical transmission channels introduce distortion including time-varying attenuation due to fading, scattering, etc., and modification of the spectral characteristics due to channel filtering and multipath effects that significantly degrade synchronization. The effects of additive noise on synchronization have been discussed in [4].

In this thesis the focus is on exploring strategies of estimation and compensation of channel distortion in order to provide levels of synchronization error acceptable for communication. A block diagram describing the channel equalization problem is

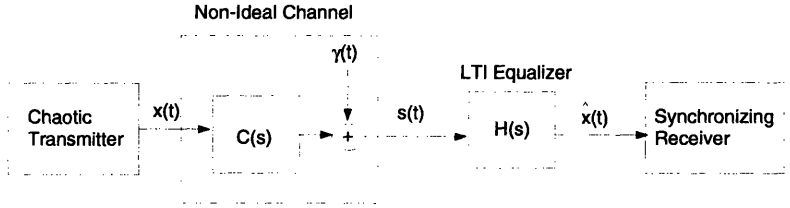

Figure 1-2: Communications with Self-Synchronizing Chaotic signals

given in Figure 1-2, where the unknown channel is given as $C(s)$, and there exists receiver noise $\gamma(t)$. Much of the experimental work described in this thesis assumes no receiver noise, however. This thesis approaches the problem from the perspective of designing the equalizing filter $H(s)$ to undo the channel filtering.

The difficulty in equalization lies in the fact that the exact input to the channel is unknown at the receiver. A solution is feasible, however, because the properties of the self-synchronizing chaotic signal are known.

The following section describes self-synchronization in more detail.

1.2 Self-Synchronization in Chaotic Systems

Self-synchronization involves a coupling of systems in which the evolution of one system is completely determined by that of another. The state trajectory of System 2 synchronizes to that of System 1, i.e. the difference between them approaches zero. The link between the pair that causes synchronization is a signal, specifically a state variable, from System 1 that serves as an input to System 2. Except for the transmission of one noise-like waveform, the two chaotic self-synchronized systems are remote from one another, which implies a potential usefulness in communications. In a communications scenario System 1 can be viewed as a transmitter, and System 2 can be viewed as a receiver.

Much of the following notation in this section is borrowed from [5]. Consider a dynamic system governed by the dynamic equations:

$$\dot{\mathbf{x}} \;=\; \mathbf{f}(t, \mathbf{x}), \quad x \in R^N. \tag{1.1}$$

The transmitter of a self-synchronizing pair evolves independently according to these equations. Its trajectory is completely described by its initial conditions.

Equation 1.1 can be partitioned into two subsets of equations, expressed as:

$$\dot{\mathbf{d}}_1 = \mathbf{D}_1(\mathbf{d}_1, \mathbf{d}_2), \quad \mathbf{d}_1 \in R^{N-m} \tag{1.2}$$

$$\dot{\mathbf{d}}_2 = \mathbf{D}_2(\mathbf{d}_1, \mathbf{d}_2), \quad \mathbf{d}_2 \in R^{m} \tag{1.3}$$

Consider duplicating $\mathbf{D}_2$ and replacing the state variables $\mathbf{d}_2$ by new state variables $\mathbf{r}$. This new system represents a receiver, whose evolution equations are:

$$\dot{\mathbf{r}} = \mathbf{D}_2(\mathbf{d}_1, \mathbf{r}), \quad \mathbf{r} \in R^{m} \tag{1.4}$$

If the subsystem represented by $\mathbf{D}_2$ is *stable* in the sense that all its the conditional Lyapunov exponents are negative, the receiver will be capable of synchronization [6]. A full treatment of what is meant by this definition of stability is given in [6]. The receiver subsystem is driven by the state variables $\mathbf{d}_1$ from the transmitter, and if stable, will synchronize to the state variables $\mathbf{d}_2$ of the transmitter.

There are a number of observations that can be made about self-synchronization. The formulation of the receiver from the transmitter equations shows that the transmitter and receiver have very similar dynamic descriptions. Another point is that there may be more than one stable decomposition of a chaotic system. Implied by that fact is the existence of a variety of receiver designs, and correspondingly a variety of synchronizing drive signals.

The work in [5, 7] details a systematic procedure for analyzing and synthesizing families of self-synchronizing chaotic systems for arbitrarily high orders. Capturing much of the typical behavior of self-synchronizing chaotic systems, the Lorenz transmitter-receiver pair is the prototype example used throughout this thesis.

1.3 Self-synchronization and the Lorenz System

Studied for decades as a simple, yet rich, example of a chaotic system, the Lorenz system has the self-synchronizing property. As we will show later, this property is the result of the global asymptotic stability of error dynamics. The Lorenz equations are given by:

$$\begin{aligned} \dot{x} &= \sigma(y-x) \\ \dot{y} &= rx - y - xz \\ \dot{z} &= xy - bz. \end{aligned} \tag{1.5}$$

x, y, and z are the transmitter state variables, and σ, r and b are constant parameters. All experiments in this thesis are performed with $\sigma = 16, r = 45.6$, and $b = 4$ for both transmitter and receiver. These parameters ensure that the system is operating in a chaotic regime.

A cascade of two stable receiver subsystems may be used to reproduce the full-dimensional behavior of the transmitter through synchronization [8]. The composite receiver dynamics are succinctly described by the Lorenz receiver equations:

$$\begin{aligned} \dot{x}_r &= \sigma(y_r - x_r) \\ \dot{y}_r &= rs(t) - y_r - s(t)z_r \\ \dot{z}_r &= s(t)y_r - bz_r. \end{aligned} \tag{1.6}$$

x_r, y_r, and z_r are the receiver state variables and $s(t)$ is the input drive signal. Note $s(t)$ replaces the occurrence of $x(t)$ in the transmitter equations. Synchronization occurs when $s(t) = x(t)$, which is confirmed by simple analysis.

Specifically, the error variables are defined as

$$e_x(t) = x(t) - x_r(t) \tag{1.7}$$

$$e_y(t) = y(t) - y_r(t) \tag{1.8}$$

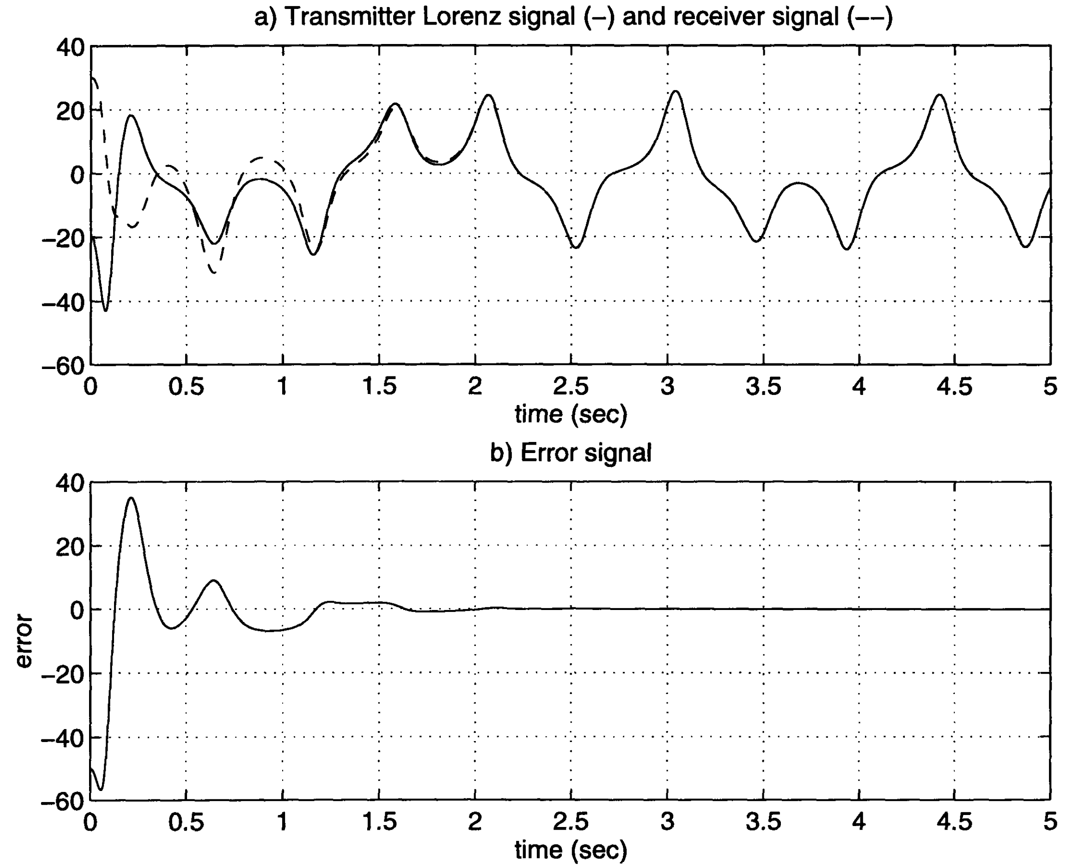

Figure 1-3: a) Lorenz drive signal and synchronizing receiver signal. b) Error signal

$$e_z(t) = z(t) - z_r(t), \tag{1.9}$$

and their evolution equations are readily derived:

$$\dot{e}_x = \sigma(e_y - e_x) \tag{1.10}$$

$$\dot{e}_y = -e_y - s(t)e_z \tag{1.11}$$

$$\dot{e}_z = s(t)e_y - s(t)e_z. \tag{1.12}$$

If $s(t) = x(t)$ the point $[0,0,0]^T$ is a globally asymptotically stable fixed point. Regardless of initial conditions of transmitter or receiver, $\mathbf{e}(t) \to 0$ as $t \to \infty$; the receiver synchronizes to the transmitter. Figure 1-3 shows synchronization for the Lorenz system occurring within about 2 seconds.

1.4 Outline of Thesis

This thesis is directed at channel estimation and equalization given the transmission of self-synchronizing chaotic signals. Figure 1-2 shows an unknown channel filter $C(s)$, and the equalizer $H(s)$ which we will attempt to design. The thesis is organized as follows.

Chapter 2 addresses implementation issues that arise when numerically integrating the transmitter and receiver equations using fourth-order Runge-Kutte integration.

In Chapter 3, we suggest equalizing strategies for both constant and time-varying gain. The first strategy is to normalize the average power of the received signal to the expected power of the self-synchronizing drive signal. Using the estimate from the average power normalization, the second strategy is adaptive error minimization. The received signal is discretized and the synchronization error is minimized at each point in time relative to an equalizing gain.

A linear time-invariant (LTI) channel model is next considered in Chapter 4 under the simplifying assumption that it is minimum phase, i.e. the stable, causal channel has a stable, causal inverse. We propose that a spectral division approach yields an excellent estimate of the channel magnitude, which is used to estimate the entire minimum phase response.

Finally in Chapter 5, we endeavor to equalize all LTI channels. We propose a solution that uses a gradient search of the synchronization error power surface relative to discrete-time FIR equalizer coefficients. By doing so, we expect to determine an equalizing filter that will minimize synchronization error.

We conclude with a chapter suggesting a potentially valuable use of self-synchronizing chaotic waveforms as test signals for system identification.

Chapter 2

Digital Implementation of Self-Synchronizing Transmitter-Receiver Pair

Throughout this thesis, we simulate the Lorenz transmitter and receiver by numerical integration of their dynamic equations to establish empirical results. We ensure repeatability and ease of simulation and analysis by performing simulations digitally.

2.1 Numerical Integration of Dynamic Equations

Given that state equations describing self-synchronizing chaotic systems are continuous-time relationships, digital integration techniques only approximate phase space trajectories. For most analysis, fourth order Runge-Kutte integration is sufficiently accurate to generate the Lorenz system trajectory. For the particular task of integrating the Lorenz transmitter-receiver pair, several implementation issues arise. They include uniform versus nonuniform step size, and composite versus decoupled implementation of the transmitter and receiver.

2.1.1 Uniform Integration Step Size

Some Runge-Kutte integration routines dynamically alter integration step size to minimize a prescribed error. The output of the routine is therefore a signal sampled at a non-uniform sampling rate. Many tools for the analysis of these signals, however, require a uniform sampling rate. For instance, a power spectral estimate of the Lorenz signal is often calculated by periodogram averaging, which uses the Fast Fourier Transform (FFT). The FFT requires uniform sampling of the signal. Also, as explained in Section 2.1.3, for the appropriate implementation of the Lorenz receiver system, the input drive signal must be oversampled by a factor of two, which is most easily done if the original signal is uniformly sampled. A uniform sampling rate is simply achieved by executing the integration with a uniform step size.

2.1.2 Composite Implementation

It is straightforward to represent a transmitter-receiver synchronized system digitally as a composite 6-dimensional system. The transmitter equations (Equations 1.5) are augmented by the receiver equations (Equations 1.6) to form the following system:

$$\begin{aligned}
\dot{x} &= \sigma(y - x) \\
\dot{y} &= rx - y - xz \\
\dot{z} &= xy - bz \\
\dot{x}_r &= \sigma(y_r - x_r) \\
\dot{y}_r &= rx - y_r - xz_r \\
\dot{z}_r &= xy_r - bz_r.
\end{aligned} \tag{2.1}$$

The "transmitted" signal, x, is actually a state variable of the 6-D system evolving independently according to the transmitter dynamics. Using this implementation, synchronization is observed. Note, however, that this implementation does not allow for degradation of the drive signal. The primary interest of this thesis is in distorting and equalizing the drive signal, for which the composite implementation is inadequate.

2.1.3 Independent Transmitter-Receiver Implementation

In this section we consider an implementation which allows for the distortion of the drive signal before being used as input to the receiver. The most flexible strategy for the simulation of the self-synchronizing system involves implementing individual routines for transmitter and receiver. The transmitter routine numerically integrates Equations 1.5, and produces the sampled Lorenz drive signal, say x_n. We are free to add noise, linearly filter, or otherwise modify the signal before using it as input to the receiver routine. Let s_n denote the modified signal. The receiver routine digitally integrates Equations 1.6 with s_n serving as an input. Synchronization will occur if $s_n = x_n$. The following discussion will describe the appropriate manner in which the receiver input s_n enters the Runge-Kutte equations.

First we must examine how Runge-Kutte integration is performed for a general system of ordinary differential equations, which are written in vector equation form as given in Equation 1.1. Given a set of initial conditions, this equation describes a path in phase space through time. The digital model only generates samples of an approximate phase path. For a particular time iteration, integration is carried out numerically by calculating a slope, multiplying it by the time step Δ and adding the resulting increment Δ_x to the existing value of x. Euler's method assigns the slope to be dx/dt directly from the state space equations. In order to guarantee numerical stability of the integration using Euler's method, the step size must be several times smaller than is required by Runge-Kutte integration. For this reason Runge-Kutte is the preferred method of integration.

Using Simpson's Rule, Runge-Kutte calculates a slope which is a weighted average of the slope at the present time t, $1/2$ a time step ahead, $t + \Delta/2$, and 1 time step ahead, $t + \Delta$.

With i denoting the successive integration steps, the Runge-Kutte equations are given by:

$$
\begin{aligned}
a &= \mathbf{f}(t_i, \mathbf{x}_i) && (2.2)\\
b &= \mathbf{f}(t_i + \Delta/2, \mathbf{x}_i + a\Delta/2) && (2.3)\\
c &= \mathbf{f}(t_i + \Delta/2, \mathbf{x}_i + b\Delta/2) && (2.4)\\
d &= \mathbf{f}(t_i + \Delta, \mathbf{x}_i + c\Delta) && (2.5)\\
\mathbf{x}_{i+1} &= \mathbf{x}_i + \Delta(a + 2b + 2c + d)/6 && (2.6)
\end{aligned}
$$

Difficulties arise in the execution of the equations by the receiver routine. Recalling the receiver equations, the right hand side is the specific function $\mathbf{f}$ for the receiver. The transmitted drive signal $s(t)$ can be viewed as an arbitrarily time varying component of the function $\mathbf{f}$. Equations 2.2-2.5 imply that the functions $\mathbf{f}(t, \mathbf{x})$ must be evaluated at 1/2 a time step, which means $s(t)$ must be evaluated at 1/2 a time step. As output from the transmitter routine, $s(t)$ is sampled only at integer time steps.

Several ways to implement the receiver routine were considered. The most elementary approach assumes $s(t)$ is constant throughout the time interval for each successive integration step; a zero order hold is performed. For each of Equations 2.2-2.5, $s(t_i) = s(t_i + \Delta/2) = s(t_i + \Delta)$. Using this algorithm the data output from the receiver routine does not show synchronization with the transmitter, because the zero-order hold contributes a 1/2 sample delay to the output of the receiver routine.

Figure 2-1 shows that implementing a zero order hold of width Δ is a filtering operation with a filter that has a constant group delay of $\Delta/2$. The magnitude modification is minimal. For instance, the requirement of stability of the receiver numerical integration dictates a sampling rate of $1/200Hz$. Most of the Lorenz signal's energy occurs from 0 to $10Hz$ (Figure 4-1). In the high frequency portion of the Lorenz spectrum ($10Hz$), magnitude attenuation from the zero-order hold filtering operation is only about $.04dB$. The Fourier transform relationship shown in Figure 2-1 indicates that a slower sampling rate will contribute to more magnitude attenuation of the drive signal.

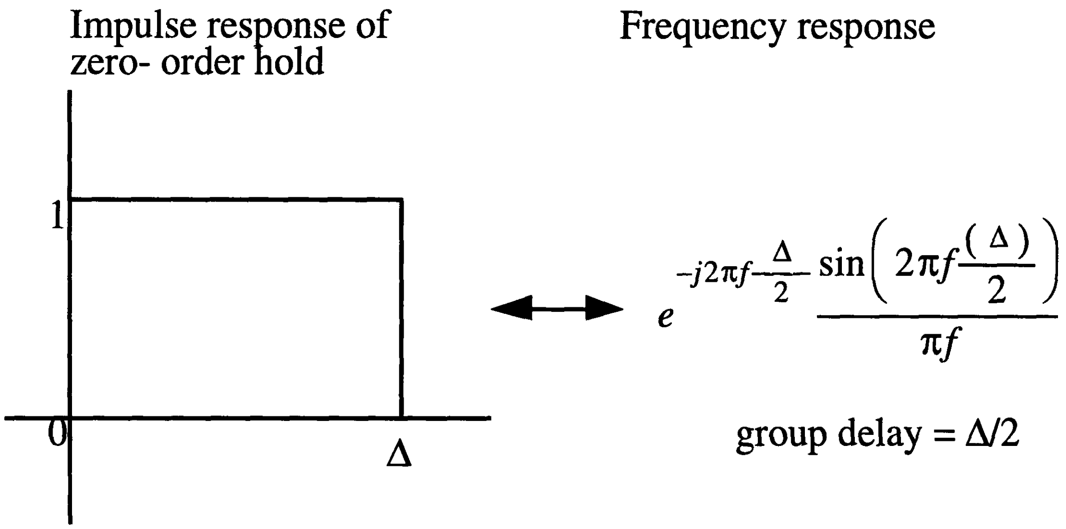
Impulse response of zero- order hold
Frequency response
1
0
Δ
$e^{-j2\pi f\frac{\Delta}{2}}\frac{\sin\left(2\pi f\left(\frac{\Delta}{2}\right)\right)}{\pi f}$
group delay = Δ/2

Figure 2-1: Impulse response and frequency response of zero-order hold

It appears from the perspective of the receiver that the drive signal has been delayed by 1/2 a time step. Therefore, the synchronized output will be delayed by the same amount. For calculation of synchronization error, it is most appropriate to compare the drive signal with the receiver output shifted back in time by 1/2 a time step.

Another approach to the integration is to input the drive signal at twice the sampling rate of that of the receiver state variables. This integration strategy does not introduce any delay into the receiver routine. The values of $s(t)$ at $t_i + \Delta/2$ and $t_i + \Delta$ are directly entered into the Runge-Kutte equations at iteration i, which implies a non-causal calculation. Oversampling the drive signal may be accomplished in one of two ways: 1) by implementing the transmitter integration with half the time step of the receiver, or 2) by keeping the transmitter and receiver time steps the same and performing band-limited interpolation before using the drive as input to the receiver routine. Either using method 1) or 2) there is no delay introduced at the receiver.

2.2 Numerical Experiments

Empirical evidence suggests that the integration procedure using the oversampled drive results in the lesser synchronization error for a clean drive compared to the

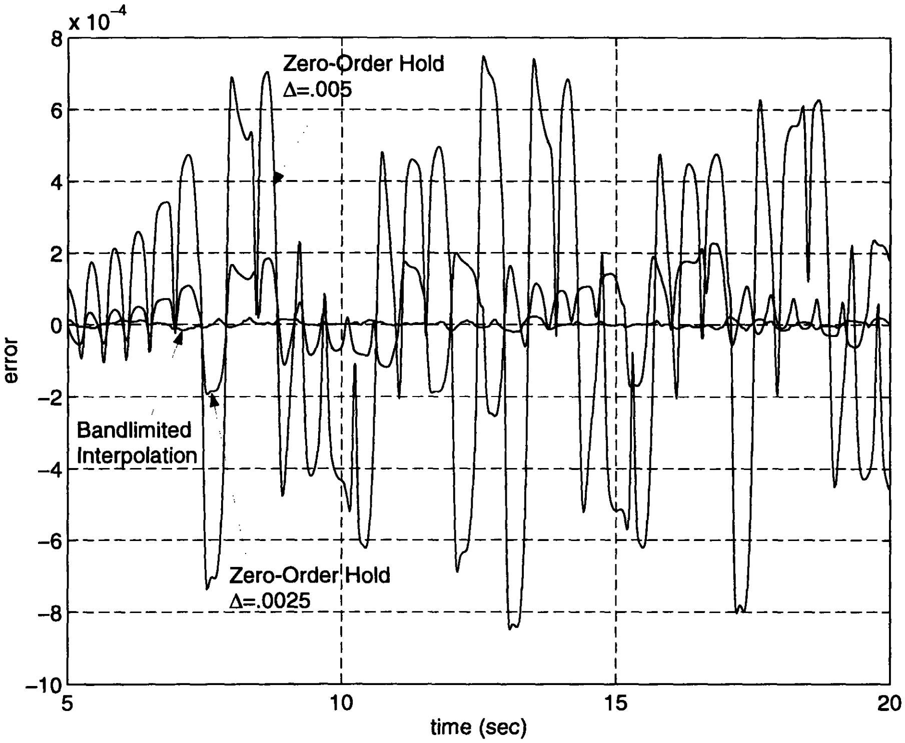

Figure 2-2: Synchronization error vs. time using zero-order hold ($\Delta = .0025, .005$) and band-limited interpolation ($\Delta = .005$) on the receiver input

zero-order hold method. The spectral magnitude modification of the zero order hold appears to degrade synchronization, and the distortion is larger for larger sampling periods. Figure 2-2 compares the calculated error trajectories for an uncorrupted drive signal using the two receiver integration approaches. The zero-order hold is performed with $\Delta = .0025$ and $\Delta = .005$. As expected the error variance increases for larger step size due to more significant magnitude attenuation at high frequencies. The band-limited interpolation method with $\Delta = .005$ achieves about an order of magnitude reduction in error over the zero order hold method.

Note that using the drive signal at twice the sampling rate, involves no more computation than simply performing a zero-order hold over a time step. If we use the zero-order hold, we must calculate the half-sample values of the the receiver input in order to compare the receiver input to the receiver output (e.g. for calculation synchronization error). This involves oversampling the receiver input by a factor of 2.

2.3 Conclusion

On the surface, Runge-Kutte integration appears to be a straightforward iterative technique. In this chapter, we have addressed some of the complexities that arise when we are integrating the equations of a self-synchronizing transmitter-receiver pair. There are two main conclusions of this chapter. First, the flexibility of the transmitter-receiver simulation is assured by implementing individual routines for transmitter and receiver. The second conclusion is that the most accurate integration of the receiver equations requires the two-times oversampling of the input drive signal.

Chapter 3

Equalization for Channel Gain

The simplest form of channel filtering is gain. In this chapter, we suggest two equalization strategies for both constant and time-varying gain. The first strategy is to normalize the average power of the received signal to the expected power of the self-synchronizing drive signal. Using the estimate from the average power normalization as a starting point, the second strategy is adaptive error minimization. The received signal is discretized and the synchronization error is minimized at each point in time relative to an equalizing gain.

3.1 Average Power Normalization

This section outlines the procedure for equalizing by normalization of the average power of the received signal to the expected power of the input signal, which is a self-synchronizing chaotic drive signal. Let $x(t)$ be the self-synchronizing chaotic drive signal. The distorted signal at the receiver is:

$$s(t) = G(t)x(t), \tag{3.1}$$

where $G(t)$ is in general a time varying gain. Figure 3-1 illustrates the loss of synchronization if $G(t) = 2$ and there is no compensation.

In order to achieve minimum synchronization error, $G(t)$ must be estimated and

$s(t)$ must be equalized on the basis of that estimate. The equalization method based on average power normalization is only valid given some assumptions.

Throughout this thesis we will be imposing an ergodicity and stationarity assumption. For a given chaotic system, a particular sample path (described entirely by initial conditions) is assumed to have the same statistics as any other sample path, and the statistics of a sample path are stationary up to second order. Therefore the expected power of the transmitter drive signal $x(t)$ has some known value, P_x. The value of P_x can be calculated at the receiver, because the receiver has the same dynamic system parameters as the transmitter. Empirical measurement of P_x over a range of initial conditions in the Lorenz system with 500 independent trials and a time window of 800 seconds resulted in an average value of 159.78, a variance of .018, a maximum of 160.16 and a minimum of 159.45.

If the power of $s(t)$ were known exactly then equalization could recover $x(t)$ exactly. A practical equalization algorithm is the following. The average power $P_s(t)$ of the gain-distorted drive signal $s(t)$ is calculated as a function of time in a sliding fixed-length window $[t-a, t+b]$ $(a > 0,\ b > 0)$.

$$P_s(t) = \frac{1}{b-a} \int_{t-a}^{t+b} s^2(\tau) d\tau. \tag{3.2}$$

Because $P_s(t)$ is only an estimate of the expected power there is estimation error in $P_s(t)$, the variance of which grows with smaller window size. Compensation is achieved by multiplying $s(t)$ by the compensating signal $Q(t)$.

$$Q(t) = \sqrt{P_x / P_s(t)} \tag{3.3}$$

$$\hat{x}(t) = s(t)Q(t) = (G(t)Q(t))x(t) \tag{3.4}$$

$\hat{x}(t)$ is then an estimate of the clean Lorenz drive. Figure 3-2(a) is a block diagram of the average power normalization strategy. For perfect synchronization, $G(t)Q(t) = 1$, but the nonzero error variance in $P_s(t)$ contributes to error in $G(t)Q(t)$. Figure 3-3 shows a sample path of $G(t)Q(t)$. In this example x(t) is a Lorenz drive signal, $G(t) = 2$ and the estimator window size is 5 seconds.

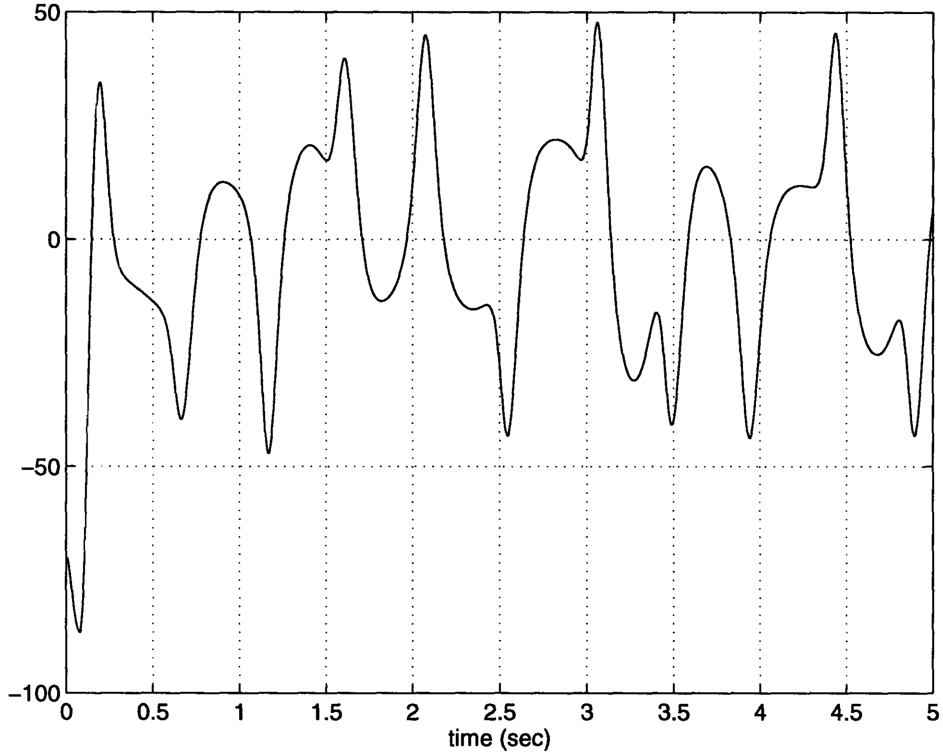

Figure 3-1: Synchronization error vs. time for $G(t) = 2$ and no compensation

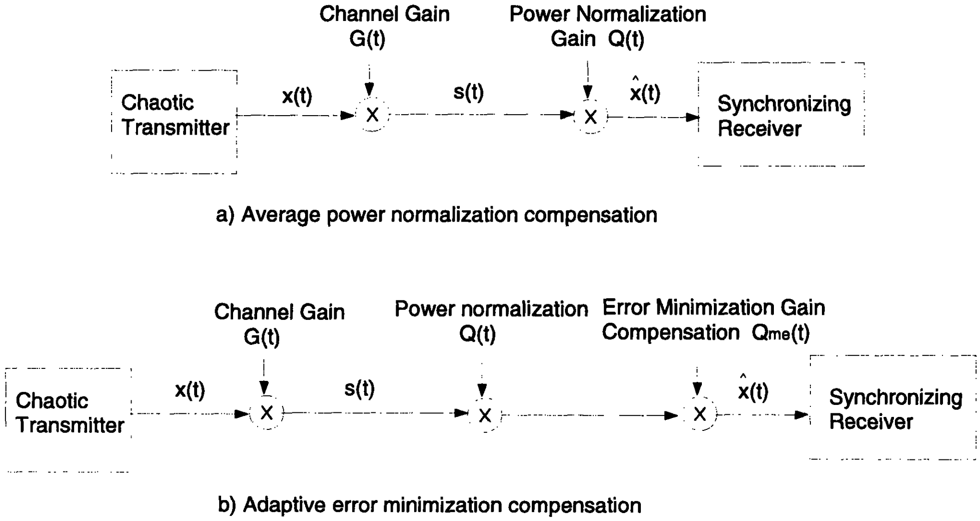
Channel Gain
G(t)
Power Normalization
Gain Q(t)
Chaotic Transmitter
x(t)
X
s(t)
X
$\hat{x}(t)$
Synchronizing Receiver
a) Average power normalization compensation
Channel Gain
G(t)
Power normalization
Q(t)
Error Minimization Gain
Compensation Qme(t)
Chaotic Transmitter
x(t)
X
s(t)
X
X
$\hat{x}(t)$
Synchronizing Receiver
b) Adaptive error minimization compensation

Figure 3-2: Block diagram of gain compensation strategy

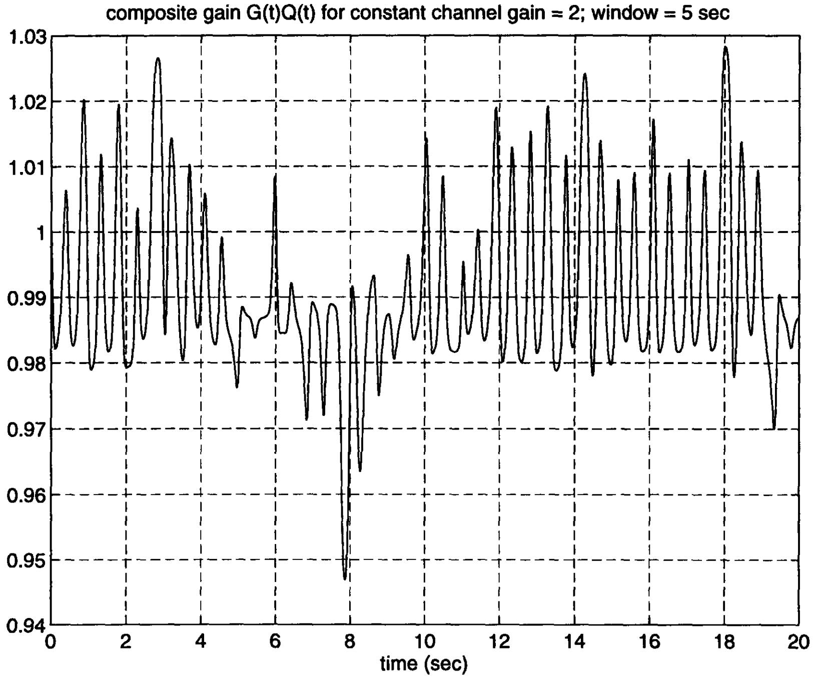

Figure 3-3: $G(t)Q(t)$ using a 5 second window for $x_r(t) = 2x(t)$, where x(t) is a Lorenz drive signal

For longer windows the product $G(t)Q(t)$ has reduced variance, as long as $G(t)$ is relatively constant within the window. Significant time variation of $G(t)$ within a window may increase the error in the power estimate. In an effort to achieve near minimum synchronization error, therefore, the window for average power normalization must be long enough to provide sufficient data for an accurate estimate, yet short enough to be avoid significantly affecting the power estimate with the time varying nature of the channel.

Self-synchronizing chaotic signals have a great deal of structure. We have exploited only a basic element of the structure which is constant expected power. The following section describes how receiver synchronization error is used to equalize more effectively given an initial estimate from average power normalization.

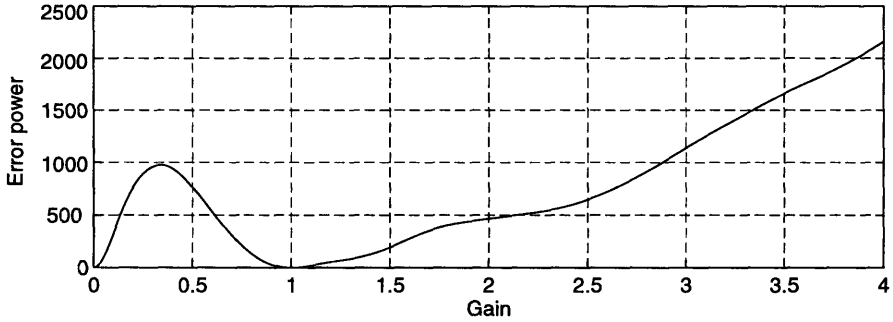

Figure 3-4: Synchronization error power vs constant gain, G

3.2 Adaptive Error Minimization

Figure 3-4 shows Lorenz system synchronization error power as a function of constant channel gain. There are two obvious minima about $G = 0$ and $G = 1$. Most significant about the curve is the unimodality for a wide range of gains about $G = 1$. In the constant gain case, given an appropriate initial channel gain estimate, a steepest descent search (gradient search) of the error power function with respect to a compensating gain should identify the compensator that achieves the minimum error. Figure 3-3 shows a $G(t)Q(t)$ for a typical constant gain channel. It varies about 1 by about $\pm.05$, which is well within the desired basin for minimum error power.

The adaptive error minimization construction is illustrated in Figure 3-2(b). The adaptive error minimization algorithm proceeds as follows. Consider a time $t = t_0$ and the signal

$$x_2(t) = Q_{me}(t_0)\ Q(t_0)\ G(t)\ x(t+t_0) \qquad -\Delta \le t \le \Delta \quad (\Delta > 0). \tag{3.5}$$

Note that the time window for $x_2(t)$ about t_0 is not necessarily the same as the window about t_0 for average power normalization. Starting with a value of 1, $Q_{me}(t_0)$ is a gain that is adjusted to achieve lowest overall synchronization error. $x_2(t)$ serves as a drive signal for the Lorenz receiver system. The algorithm minimizes the error with respect to $Q_{me}(t_0)$. If the algorithm is performed for all t_0, a new equalizing gain signal, $Q_{me}(t)Q(t)$, is created.

Again, how well $Q_{me}(t)Q(t)$ equalizes $G(t)$ depends on the window size, 2Δ. The window must be large enough so that $x_2(t)$ is a representative waveform of the self-synchronizing drive signals, and also large enough so that the transient error is not a significant portion of the error signal. In fact, the transient error should not be included in any average error power calculation during the steepest descent search. The window must also contain enough data such that the estimate of the error power at a particular point on the error power function has sufficiently small variance.

The primary reason for keeping the window small is to ensure that $G(t)$, is relatively constant within a window. The behavior shown in Figure 3-4 only describes a relationship between error power and a *constant* gain G. If $G(t)$ is significantly time varying within a window, the estimate of the channel gain at t_0 may not be the same as the estimate for $G(t)$ constant. The estimate may in fact be worse than the estimate using average power normalization. So when $G(t)$ is time varying, the composite gain of the channel equalizer cascade, $Q_{me}(t)Q(t)G(t)$ may vary more from unity than than $Q(t)G(t)$. Use of adaptive error minimization after average power normalization is therefore advisable only under certain, more placid channel conditions.

The effects of a time-varying gain on equalization is very difficult to quantify for an arbitrary $G(t)$. If, however, we consider a linear approximation of $G(t)$ within a window, the analysis becomes more tractable. The following two sections discuss the effect of the linearly time-varying gain on the two equalizers. Section 3.3 shows that compared to the constant channel gain case, the average power normalization power estimate is relatively unaffected by a small slope linear channel gain. Section 3.4 argues that the linearly varying gain biases the adaptive error minimization equalizer. The degree to which it is biased is unknown, however. Numerical experiments in Section 3.5 show that adaptive error minimization can actually worsen the equalization of the average power normalization in the time-varying gain case.

3.3 Effect of Linearly Varying Gain on Average Power Equalization

Consider a situation in which the distortion of a chaotic drive signal is caused by a linearly varying gain. For a time window about time t_0, $[t_0 - \Delta, t_0 + \Delta]$, the time-varying gain is $G_L(t) = K + \frac{\epsilon}{\Delta}(t - t_0)$. K is the channel gain for $t = t_0$ and ϵ is the maximum deviation of $G(t)$ from K in the window. Appendix A shows that to the first order (in ϵ), the mean and variance of the power estimate for the linearly varying channel gain is approximately equal to that for the constant gain case, $G(t) = K$. So for strictly increasing or strictly decreasing channel gains of small slope, the average power normalization should reduce synchronization error nearly as effectively as for constant gain.

In the next section we will show that the gain estimate made by the adaptive error minimization actually worsens with time varying channel gain.

3.4 Effect of Linearly Varying Gain on Adaptive Error Minimization Equalization

For the linearly time-varying gain channel, the performance of the adaptive error minimization is less analytically tractable than that of the average power normalization. We will use approximate arguments with empirical support to attempt to explain the behavior.

We will assume that the receiver synchronization is rapid relative to the rate of change of the channel gain. Therefore, if the gain $Q_{me}(t_0)\ Q(t_0)\ G(t)$ is unity at any time in the window $t_0 - \Delta \leq t \leq t_0 + \Delta$ then the synchronization error power is approximately zero at that time. With this assumption and the fact that error power is a continuous function of the gain, it is reasonable to assume that the gradient search of the error power curve will yield a gain $Q_{me}(t_0)\ Q(t_0)\ G(t_0)$ that is close to unity.

For the purposes of illustration, we next consider the experiment in which the Lorenz drive signal passes through a channel gain $G(t) = 1 - (t - 10)/20$, shown in Figure 3-5(a). Consider the window $0 \leq t \leq 20$ which is centered about $t = 10$. The channel has a gain of one at $t = 10$ seconds. The channel needs no gain compensation at $t = 10$, i.e. the equalizing gain $Q_{me}(10)Q(10)$ should equal 1.

As we expect, Figure 3-5(b) shows the error power is zero at $t = 10$ seconds. The figure also shows the envelope that contains the error in the region for which $G(t) > 1$. The envelope does not bound the error signal in the region for which $G(t) < 1$, revealing an asymmetry of the error signal amplitude about the zero error point $t = 10$ seconds. In the experiment, the error minimization routine is affected by this asymmetry and yields $Q_{me}(10)Q(10) = 1.16$. Figures 3-5(c) and (d) indicate an explanation for this overestimation. Figure 3-5(c) shows that $Q_{me}(10)Q(10)G(t)$ is essentially the channel gain curve shifted forward in time by 3 seconds; the slope is also slightly changed. The gain $Q_{me}(10)Q(10)G(t)$ is greater than unity for a majority of the time window (about 13 seconds), while the gain is less than unity for about 7 seconds. Figure 3-5(d) shows the effect that this compensated gain has on the error signal. The error envelope is essentially shifted relative to that for no compensation (Figure 3-5(b)). The error has a more even amplitude across the window, so that a minimum error power is achieved.

The above arguments suggest that the reduction of overall synchronization error by adaptive error minimization is compromised by time varying channel gain. Given that the average power normalization gain estimate is somewhat robust to time varying gain, it may be better than adaptive error minimization at reducing synchronization error in some cases. The following section empirically compares the two strategies of gain compensation for constant and time-varying channel gains.

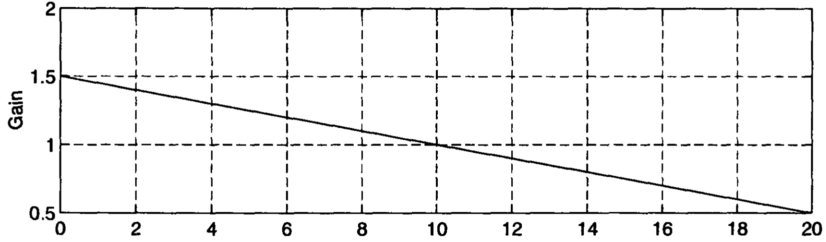
(a) Channel gain, G(t)=1-(t-10)/20

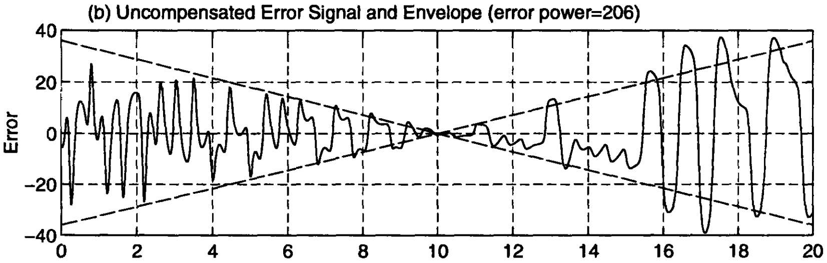
(b) Uncompensated Error Signal and Envelope (error power=206)

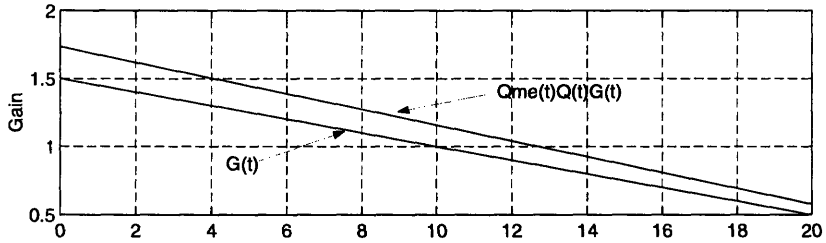
(c) G(t)=1-(t-10)/20, Qme(t)Q(t)G(t)=1.16 G(t)

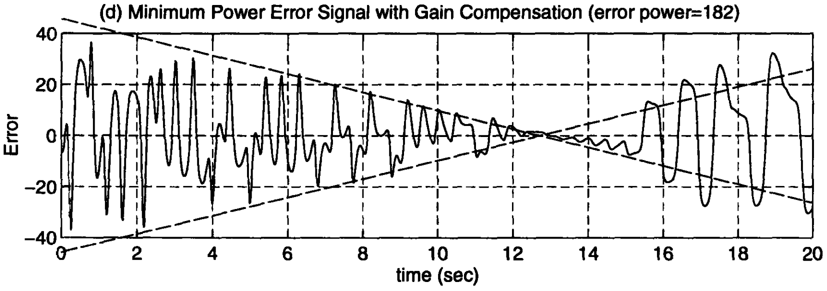
(d) Minimum Power Error Signal with Gain Compensation (error power=182)

Figure 3-5: (a) Time varying gain $G(t) = 1 - (t - 10)/20$, (b) Corresponding synchronization error versus time, (c) Minimum error Gain $Q_{me}(10)Q(10)G(t)$, (d) Error corresponding to gain in (c)

3.5 Numerical Experiments: Comparison of Average Power Normalization and Adaptive Error Minimization

This section will discuss two experiments, one involving a constant gain channel and the other involving a linearly time-varying channel. We will compare how effectively the two strategies, *average power normalization* and *adaptive error minimization*, equalize these gains.

These experiments again involve the Lorenz transmitter-receiver pair, with the parameter values described in Section 1.3. The Lorenz equations were numerically integrated using a fourth order Runge-Kutte method with a fixed step size of .005. The corresponding sampling period of the received signal is $T = .005$.

For a constant gain of $G(t) = 2$ and estimator window of 20 seconds, Figure 3-6 shows the synchronization error versus time after equalization using both compensating strategies: average power normalization and adaptive error minimization. Clearly both compensators show reduced error compared to no compensation (Figure 3-1). Also the adaptive error minimization has reduced the error by at least an order of magnitude over the average power normalization. For relatively constant gain channels there is significant improvement in synchronization error by taking the extra equalization step of adaptively minimizing error.

Again comparing both compensating strategies, Figure 3-7 shows the synchronization error versus time after equalizing a channel with time-varying gain $G(t) = 1 + t/10$. Note that the gain variation within the 20 second window is significant, ranging from 1 to 3. The results are quite the opposite of the previous experiment. There is an increase in error power for both strategies compared to the constant gain case. But most significant about the experiment is that equalization with adaptive error minimization actually increases synchronization error over the average power normalization. This example shows that adaptive minimization is not the optimum method for synchronization error reduction for some time varying channel gains.

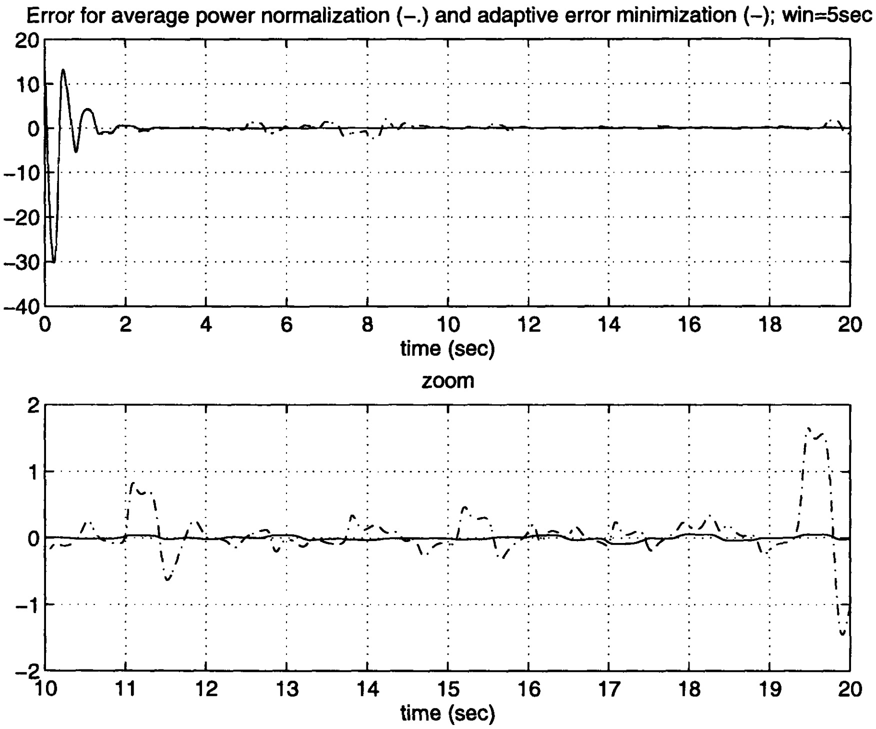

Figure 3-6: Synchronization error reduction after equalization of constant gain channel. $G(t) = 2$.

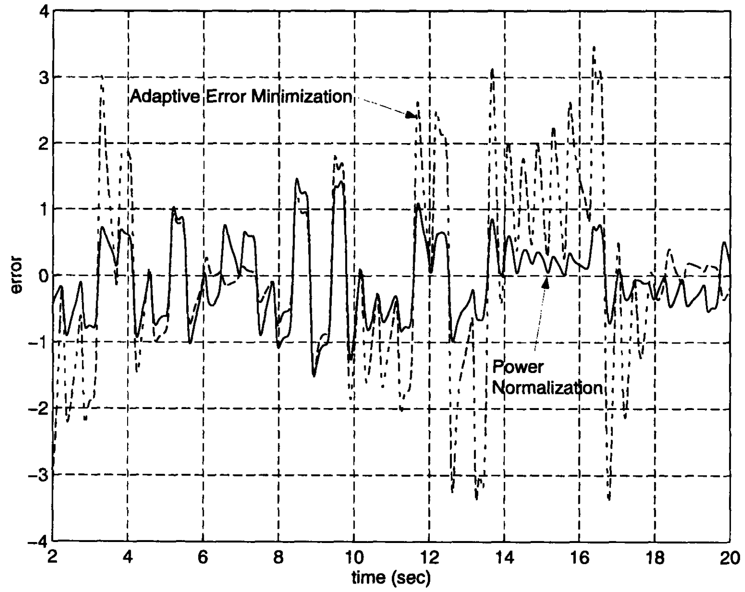

Figure 3-7: Synchronization error after equalization of time varying gain channel. $G(t) = 1 + t/10$.

3.6 Conclusion

This chapter outlined two strategies for equalization of channel gains for communications with self-synchronizing chaotic signals. *Average power normalization* exploits the assumption of a stationary average power of the input chaotic drive signal. This strategy simply normalizes the power received from the channel by the power expected from the self-synchronizing chaotic drive. It was shown that for linearly varying gain, the gain estimate by average power normalization has approximately the same mean and variance as for the constant gain case.

For relatively constant gain channels, a second equalization procedure, *adaptive error minimization* can improve upon the equalizing estimate of average power normalization. This method utilizes the self-synchronizing property of the receiver and the unimodality of the error power versus gain curve to attempt to achieve minimum overall error. We have provided experimental evidence which demonstrates that adaptive error minimization used when the channel gain is relatively constant reduces the error significantly more than adaptive power normalization. We have also experimentally shown that adaptive error minimization actually worsens the average power normalization if the channel gain is sufficiently time-varying.

Chapter 4

Equalization of Minimum Phase Channels

4.1 Introduction

Linear time invariant (LTI) channel equalization is first addressed under the simplifying assumption that the channel is minimum phase, i.e. the channel is stable and causal and has a stable and causal inverse. If a filter is minimum phase, its magnitude and phase are uniquely related. A discrete-time minimum phase filter has all of its poles and zeros inside the unit circle. The phase of the filter, therefore, is completely determined by the magnitude through a Hilbert transform relationship. For a discrete time channel $C(z)$ the relationship is:

$$arg[C(e^{j\omega})] = -\frac{1}{2\pi}\mathcal{P}\int_{-\pi}^{\pi} log|C(e^{j\omega})|cot(\frac{\omega-\theta}{2})d\theta \tag{4.1}$$

This chapter will first describe how to estimate the channel magnitude by spectral division. We next discuss some of the techniques for determining the minimum phase equalizing filter impulse response from the magnitude estimate. Finally, there is a section on numerical experiments in which a Lorenz drive signal serves as input to a lowpass minimum phase channel and is equalized.

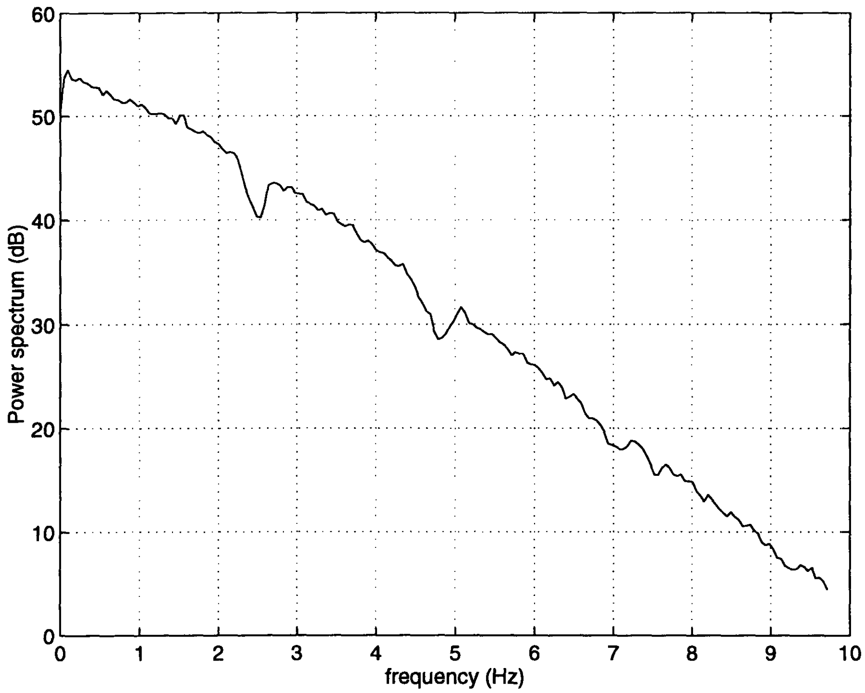

Figure 4-1: Power spectrum of Lorenz signal

4.2 Power Spectral Division

It is convenient to view trajectories of a chaotic system as sample paths of a random process. Because the signals are the output of a completely deterministic system, this model is not strictly accurate, but it allows the application of techniques that meaningfully characterize the signals. We also impose further assumptions of stationarity and ergodicity.

The first assumption is that the self-synchronizing chaotic drive is wide sense stationary, which specifies that the mean is independent of time and the autocorrelation function is shift-invariant. Second, the drive is assumed ergodic, i.e. all sample paths are probabilistically the same. Each sample path is specified by an initial condition. Stationarity and ergodicity are typically true of self-synchronizing chaotic systems [9, 5]. Given these properties, the input chaotic power spectrum, $P_{xx}(j\omega)$, exists and is known at the receiver, because the receiver dynamics are the same as the transmitter dynamics. Figure 4-1 shows the Lorenz spectrum determined by an averaged periodogram estimator.

Knowledge of the power spectrum of the input and output of a channel gives a straightforward solution for the channel magnitude response. Figure 1-2 shows the non-ideal transmission channel composed of the linear filter $C(s)$ and an additive noise source $\gamma(t)$ at the receiver end. $P_{ss}(j\omega)$ is the power spectrum of the received signal and is given by

$$P_{ss}(j\omega) = P_{xx}(j\omega)|C(j\omega)|^2 + P\gamma\gamma(j\omega), \tag{4.2}$$

where $P\gamma\gamma(j\omega)$ is the power spectrum of the noise signal $\gamma(t)$. The input to the receiver system is the compensated drive signal $\hat{x}(t)$. Because its power spectrum is given by

$$P_{\hat{x}\hat{x}}(j\omega) = P_{ss}(j\omega)|H(j\omega)|^2. \tag{4.3}$$

$|H(j\omega)|^2$ is chosen to be a quotient of known quantities:

$$|H(j\omega)|^2 = \frac{P_{xx}(j\omega)}{P_{ss}(j\omega)}. \tag{4.4}$$

This choice ensures that the power spectrum of the equalized drive signal closely approximates that of the transmitted drive signal. In general the phase of the equalizer is unrelated to the magnitude. If we assume, however, that the channel is minimum phase, the equalizer is also minimum phase, and the phase response of the equalizer is uniquely determined by its magnitude. To derive the phase response from the magnitude response, a variety of techniques may be used such as the autocorrelation method of linear prediction (all-pole modeling), spectral factorization, or Hilbert transform methods.

4.3 Minimum Phase Filter Response from Band-limited Magnitude

One point of note about the spectral division of Equation 4.4 is that the power spectrum of the chaotic drive signal is band limited. Figure 4-1 shows the Lorenz power spectrum highly attenuated at high frequency. Outside of a particular band of frequencies, the input to the channel $C(s)$ has virtually no energy; there is no excitation from which to obtain magnitude information. The band-limited nature of the input leads to an ill-conditioning of the spectral division. Only a particular band of the channel's magnitude response is known with reasonable certainty. Figure 4-3 shows an example of the ill-conditioned estimate of the magnitude of a lowpass channel. The channel in this case is a third order Butterworth filter.

In order to recover the input drive signal, channel inversion is only necessary in the band where the drive has energy. But most minimum phase impulse response derivations require full-band knowledge of the magnitude response. We will illustrate the need for full-band knowledge and the possible solutions using only partial band information by considering the example of all-pole modeling [10].

All-pole modeling is a discrete time algorithm that assumes an all-pole model for a channel whose impulse response is c_n. The z-transform of c_n is $C(z)$. There exists an FIR inverting filter $a_n = 1, a_1, a_2, ..., a_N$ of length $N+1$. Let $A(z)$ be the z-transform of a_n. The solution for a_n minimizes the squared error term:

$$E_N = \sum_{n=0}^{L} e_n^2 \tag{4.5}$$

where $e_n = c_n * a_n - \delta_n$ and $L > N$. $c_n * a_n$ represents the convolution of c_n and a_n, and δ_n is the unit impulse. It follows that a_n whitens c_n to form an approximation of δ_n.

This problem formulation requires the solution of the *autocorrelation normal equations*:

$$\begin{bmatrix} -r_1 \\ -r_2 \\ \vdots \\ -r_{N+1} \end{bmatrix} = \begin{bmatrix} r_0 & \cdots & r_{N+1} \\ r_1 & \cdots & r_N \\ \vdots & \cdots & \vdots \\ r_{N-1} & \cdots & r_0 \end{bmatrix} \begin{bmatrix} a_1 \\ a_2 \\ \vdots \\ a_N \end{bmatrix}$$

where $r_n = c_n * c_{-n}$ is the autocorrelation function of the filter being modeled. Clearly

r_n is the inverse discrete-time Fourier transform of $|C(e^{j\omega})|^2$. In order to perform the transform, we need to know the value of $|C(e^{j\omega})|^2$ for all frequencies $-\pi$ to π.

There are several ways to approach the problem of knowing only partial band information. Let $|C(e^{j\omega})|^2$ be known in the band $-\omega_c < \omega < \omega_c$, $0 < \omega_c < \pi$. One solution is to create a function $\tilde{R}(j\omega)$, which is $|C(e^{j\omega})|^2$ scaled in frequency:

$$\tilde{R}(j\omega) = |C(e^{j\omega(\omega_c/\pi)})|^2 \qquad -\pi \leq \omega \leq \pi. \tag{4.6}$$

We have effectively mapped ω_c out to π. In the time domain, this has the effect of lowpass filtering r_n with a filter of cutoff ω_c and downsampling the resultant signal by π/ω_c. The new magnitude function $\tilde{R}(j\omega)$ is known from $-\pi$ to π, and its inverse transform, say $\tilde{r}_n$, can be determined. The equalizer solution to the normal equations using $\tilde{r}_n$, denoted by $\tilde{a}_n$, will also be downsampled by π/ω_c. To determine a_n, we must perform band-limited interpolation on $\tilde{a}_n$ with an upsampling factor of π/ω_c.

Another solution to the partial band magnitude knowledge issue is given in [11]. The authors suggest retaining known and unknown frequency bands, and iteratively extrapolating the channel magnitude into the unknown bands by a method described in [11]. Once there exists a satisfactory estimate of the full band magnitude estimate, all-pole modeling or other techniques can be used to obtain the minimum phase equalizer.

4.4 Numerical Experiments

This section discusses an experiment in which there is a minimum phase channel with a lowpass characteristic that corrupts the synchronization of the Lorenz receiver. With the apriori knowledge that the channel is minimum phase, we equalize with a minimum phase equalizer determined from a magnitude estimate.

These experiments again involve the Lorenz transmitter-receiver pair, with the parameter values described in Section 1.3. The Lorenz equations were numerically integrated using a fourth order Runge-Kutte method with a fixed step size of .005.

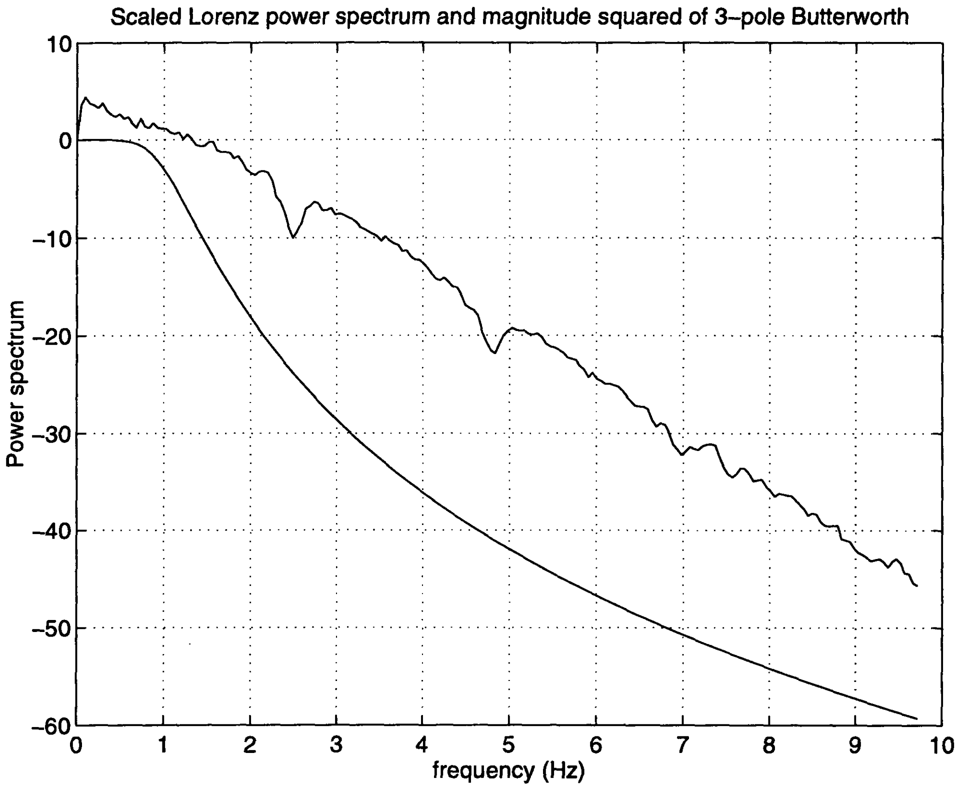

Figure 4-2: Power spectra of Butterworth channel and scaled Lorenz signal

The corresponding sampling period of the received signal is $T = .005$. The sampled Lorenz drive is denoted x_n.

In the experiment we chose the channel filter $C(z)$ to be a discrete-time Butterworth. In order to minimize the complexity of the experiment the receiver noise $\gamma(t)$ is assumed zero. $C(z)$ is a 3-pole Butterworth with a cutoff frequency at 1 Hz. Figure 4-2 shows the frequency response of $C(j\omega)$ and the superimposed Lorenz power spectrum. There is obvious attenuation of the Lorenz signal in a high energy portion of its spectrum. The corrupting effects of filtering on synchronization are shown in Figure 4-4(a), where synchronization error is shown to be on the order of the input Lorenz signal. The chaos to error ratio [5] is about 0dB, which is unacceptable for any communication scheme.

Figure 4-3 shows that spectral division yields a very accurate estimate of the channel magnitude out to about 17 Hz. The spectral estimates used in Equation 4.4 are obtained by periodogram averaging of the sampled signals x_n and s_n, the

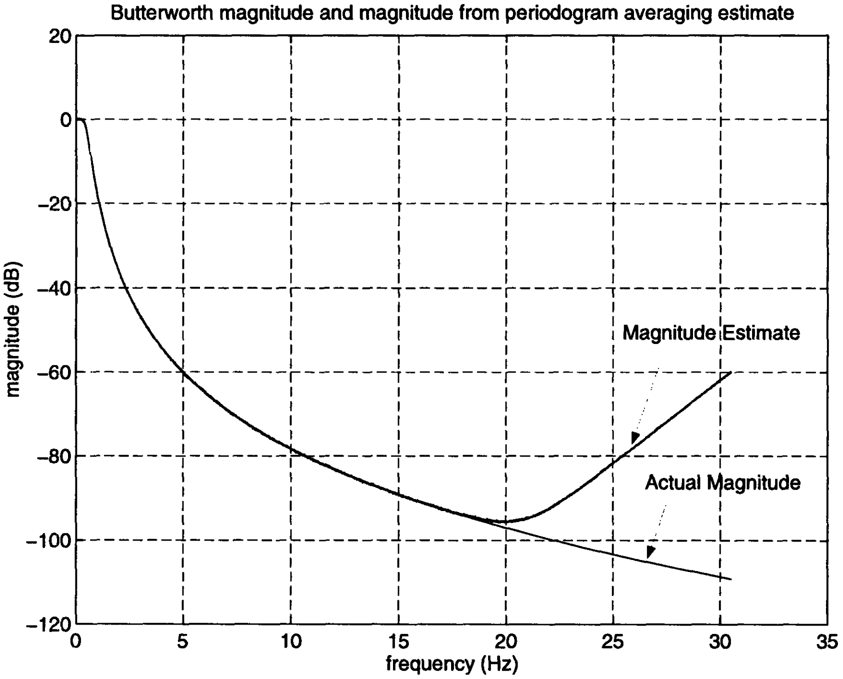

Figure 4-3: Actual and Estimated magnitude of Butterworth channel

sampled input and sampled output respectively. The Lorenz power spectrum $P_{xx}(j\omega)$ is calculable offline, and is the same for every channel estimate calculation. The effects of the ill-conditioning of the spectral division are obvious beyond 17 Hz.

For this experiment all-pole modeling is applied to the magnitude estimate out to 16 Hz to determine an equalizing filter. The frequency 16 Hz is mapped to the discrete-time frequency π to give a full band representation of the spectrum. All-pole modeling assumes a fixed order inverting filter. In any implementation of the algorithm, the filter order must be chosen sufficiently large to undo any minimum phase channel between transmitter and receiver that is typical for a particular application. In this experiment the order is 20.

A comparison of synchronization error for unequalized and equalized receiver systems is shown in Figure 4-4. The chaos-to-error ratio after equalization is 33dB, which is at a reasonably acceptable level for communication.

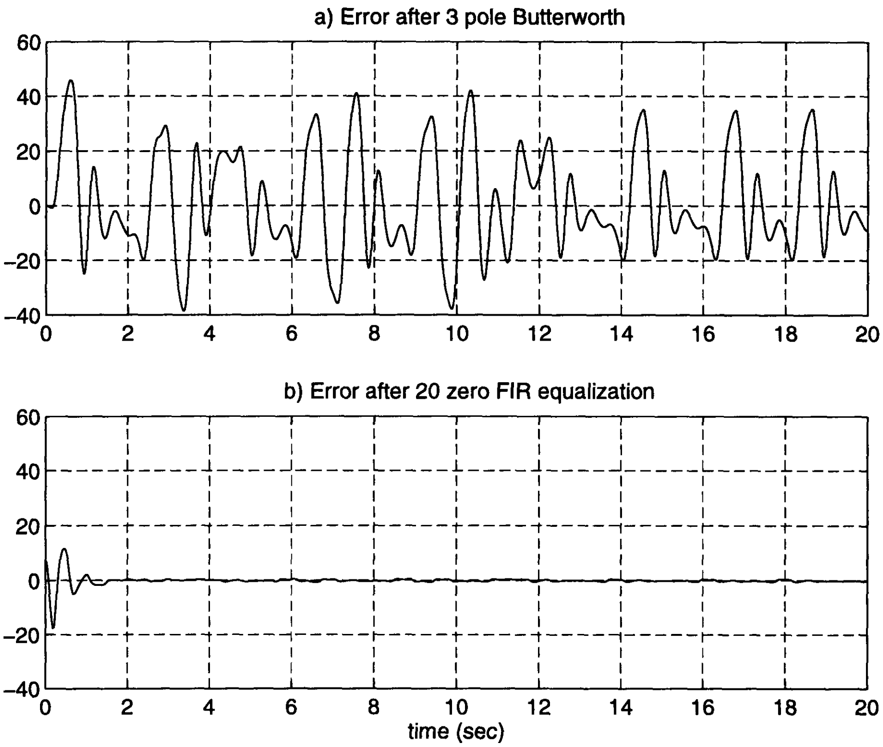

Figure 4-4: Error versus time for Butterworth channel. a) without compensation, b) with compensation

4.5 Conclusion

Channel magnitude estimation with chaotic self-synchronizing signals is straightforward using spectral division. No method of estimation will estimate magnitude outside of the nonzero energy band of the Lorenz drive signal, but we need to equalize the signal only at the frequencies where it has energy. Our empirical results show that spectral division provides an accurate estimate of the channel magnitude. With the prior assurance that the channel is minimum phase, equalization is carried out easily using the magnitude information.

The assumption of minimum phase however is often not appropriate, and the method described in this chapter is not well suited for non-minimum phase equalization. For instance, an all-pass channel needs no magnitude compensation, but contributes to significant loss of synchronization. Phase plays an important role in chaotic transmitter-receiver synchronization. In the next chapter we develop new strategies that better address phase equalization. In this chapter we have utilized some general statistical characteristics of the chaotic drive signals. We next take advantage of a fundamental property of the receiver systems that we are studying: self-synchronization.

Chapter 5

Equalization of Linear Time Invariant Channels

5.1 Introduction

In this chapter we suggest an approach for equalizing linear time invariant channels of arbitrary magnitude and phase responses. Chaotic synchronization is affected by both magnitude and phase. For instance, synchronization is corrupted by gain channels (purely magnitude modification) and all-pass channels (purely phase modification). Clearly a minimum phase or other arbitrary phase assumption will not sufficiently diminish synchronization error caused by an arbitrary LTI channel. We intend to exploit the self-synchronization property of the receiver to compensate for both magnitude and phase.

The objective of channel compensation is to minimize error between transmitter and receiver, which is equivalent to minimizing synchronization error at the receiver. Minimum synchronization error will only be achieved with optimal *magnitude* and *phase* inversion by the equalizer. We propose a method in which the compensating filter parameters are adjusted in a systematic fashion, modifying both magnitude and phase, such that minimum synchronization error will be achieved. Figure 5-1 shows a block diagram for this strategy which involves feedback of the synchronization error to adjust the filter parameters.

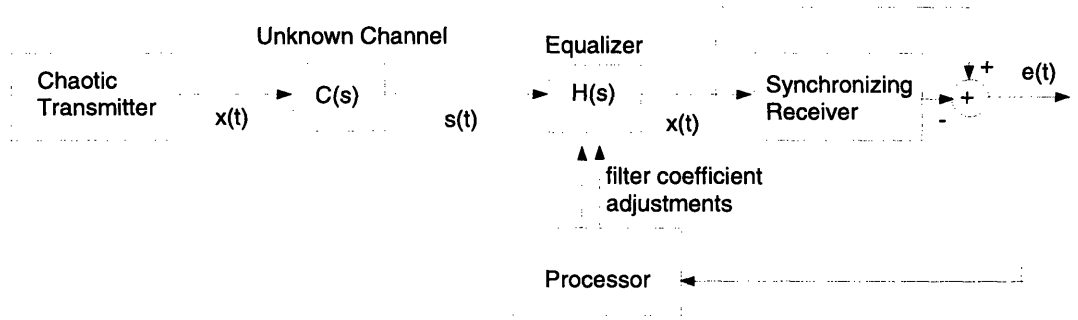
Unknown Channel
Equalizer
Chaotic Transmitter
x(t)
C(s)
s(t)
H(s)
x(t)
Synchronizing Receiver
+
e(t)
+
-
filter coefficient adjustments
Processor

Figure 5-1: Steepest Descent Implementation for an FIR equalizer

5.2 The Error Power Surface

Referring to Figure 5-1 the received corrupted drive signal is $s(t)$. Consider $s(t)$ sampled above the Nyquist rate; the discrete signal is denoted by s_n, $n = 1, 2, \ldots, M$. Assume the equalizer is implemented as a length N discrete time FIR filter, h_n, $n = 1, 2, \ldots, N$. In general N is much less than M. For an arbitrary set of FIR coefficients we generate an approximation $\hat{x}_n$, $n = N, \ldots, M$ that is input to the receiver, and there is a corresponding error signal and average error power. The average error power is a function of the N equalizer coefficients. There exists an N dimensional error power surface of which we wish to find a minimum. An appropriate strategy for finding the minimum is a steepest descent method [12].

5.3 Steepest Descent Implementation

$\hat{x}_n$ is the result of a convolution operation between s_n and h_n, described algebraically as

$$\begin{bmatrix} \hat{x}_N \\ \hat{x}_{N+1} \\ \vdots \\ \hat{x}_M \end{bmatrix} = \begin{bmatrix} s_1 & \cdots & s_N \\ s_2 & \cdots & s_{N+1} \\ \vdots & \cdots & \vdots \\ s_{M-N+1} & \cdots & s_M \end{bmatrix} \begin{bmatrix} h_N \\ \vdots \\ h_2 \\ h_1 \end{bmatrix}$$

or, using vector notation, as

$$\hat{\mathbf{x}} = S\mathbf{h} \ . \tag{5.1}$$

Given adequate inversion of the channel, $\hat{\mathbf{x}}$ closely approximates the input self-synchronizing drive signal, which implies $\hat{\mathbf{x}} \approx \mathbf{r}$ where $\mathbf{r} = (r_N, \ldots, r_M)^T$ is the receiver output. In order to explicitly show the dependence on the equalizer impulse response, $\mathbf{h}$, the notation for the receiver output will be $\mathbf{r}(\mathbf{h})$. The expression for the squared synchronization error is thus

$$J = (S\mathbf{h} - \mathbf{r}(\mathbf{h}))^T (S\mathbf{h} - \mathbf{r}(\mathbf{h})). \tag{5.2}$$

A gradient descent iteration is implemented by the following equation

$$\mathbf{h}_{i+1} = \mathbf{h}_i - \gamma_i \frac{\nabla J}{||\nabla J||} \ , \tag{5.3}$$

where γ_i is an appropriate step size for the i^{th} iteration. This approach involves computing the gradient of J at the i^{th} iteration of $\mathbf{h}$, say $\mathbf{h}_i$, and then updating the estimate of $\mathbf{h}$ by moving it in the direction of steepest descent of J.

The gradient of J is straightforward to calculate and is given by

$$\nabla J = 2(S^T - \nabla \mathbf{r}(\mathbf{h}_i))(S\mathbf{h}_i - \mathbf{r}(\mathbf{h}_i)) \ , \tag{5.4}$$

where $\nabla \mathbf{r}(\mathbf{h}_i)$ denotes the Jacobian of $\mathbf{r}(\mathbf{h})$ evaluated at $\mathbf{h}_i$. This matrix is easily estimated numerically by perturbing the components of $\mathbf{h}_i$ and measuring the resulting change in the receiver output.

It is important to choose a suitable γ_i for efficient descent. We use the *golden-section search* algorithm, which selects the step size that results in the largest reduction of J at each iteration. The algorithm then simply minimizes J along one-dimensional cross-sections at each iteration. Each cross-section is in the direction of the gradient at the particular iteration.

5.4 Starting Point for the Steepest Descent Iteration: Initial Equalizer Estimate

The gradient descent iteration requires an initial estimate of the equalizer transfer function, $\mathbf{h}_0$. An appropriate choice is the minimum phase solution as determined in the previous chapter. The channel magnitude is appropriately equalized, and at this stage there exists no phase information that would allow a better initial estimate.

There exists, however, some troubling features of this initial estimate that are immediately apparent. Assume for simplicity, exact magnitude equalization. Any improvement in phase equalization must occur at the expense of a loss in magnitude equalization. It seems likely therefore that there may occur a local minimum in the error power surface, where the decrease in synchronization error due to better phase equalization is just exceeded by an increase in error due to worsening magnitude equalization. In the presence of local minima, the steepest descent algorithm may converge on a local, not global minimum. We hope to converge on the global minimum.

An initial estimate that is minimum phase also causes another, perhaps more serious problem. A minimum phase starting point will tend to cause convergence to a local minimum solution that is also minimum phase. The reasoning is quite simple. In order for the FIR equalizer to converge on a *non-minimum phase* solution from a minimum phase starting point, at least one of its zeros must cross from the inside of the unit circle to the outside of the unit circle.

We will evaluate the plausibility of any iteration crossing the unit circle by considering the effect on group delay of two filter configurations: 1) a zero just inside the unit circle, and 2) a zero just outside the unit circle. A zero just inside the unit circle will contribute a *large negative* group delay at its local frequency, and a zero just outside the unit circle will contribute a *large positive* group delay.

Now consider a zero as it approaches the unit circle from an interior location. It is decreasing the quadratic function J by making the group delay at its local frequency more negative. If the zero were to move across the unit circle, not only would the group delay stop becoming more negative, but it would become highly positive. Since the function J was initially decreasing with increasingly negative group delay, it is highly unlikely that it will decrease any further with a largely positive group delay. It is therefore unlikely that a zero will cross from the inside of the unit circle to the outside. This means that a minimum phase starting point will likely yield a minimum phase solution to the error power minimization. Experiments have empirically confirmed this hypothesis.

The above discussion suggests that we will be constrained to equalize all LTI channels with minimum phase compensators, a subset of all FIR compensators. Thus we will probably not find the globally optimum equalizer solution. In the next section we propose a solution that will attempt to find the global optimum.

5.5 Exhaustive Search of Initial Equalizer Zero Placements

This section will suggest a logical approach to expand the convergence set of the equalizer optimization to include minimum phase and non-minimum phase equalizers. In the previous section, the initial equalizer for the steepest descent algorithm was chosen to equalize the magnitude very well, but its phase was arbitrarily chosen to be that of the minimum phase filter. In this section we take advantage of the fact that, for FIR filters of order N there exist exactly 2^N filters with equal magnitude responses. We show why this is true below.

Consider an arbitrary minimum phase N^{th} order filter. The magnitude response will be unchanged by filtering by a first order all-pass, with a pole at α and a zero at $1/\alpha^*$. If the pole of the all-pass cancels a zero of the original minimum phase equalizer, the resulting cascade is again an N^{th} order FIR filter, but with a new non-minimum phase zero at $1/\alpha^*$. Consider the N zeros of the original FIR filter. Each zero α_i, $i = 1, 2, ..., N$, can be replaced by a zero at $1/\alpha_i^*$, and the magnitude is unchanged. There are 2 allowable locations per zero, and therefore there are 2^N distinct filters of

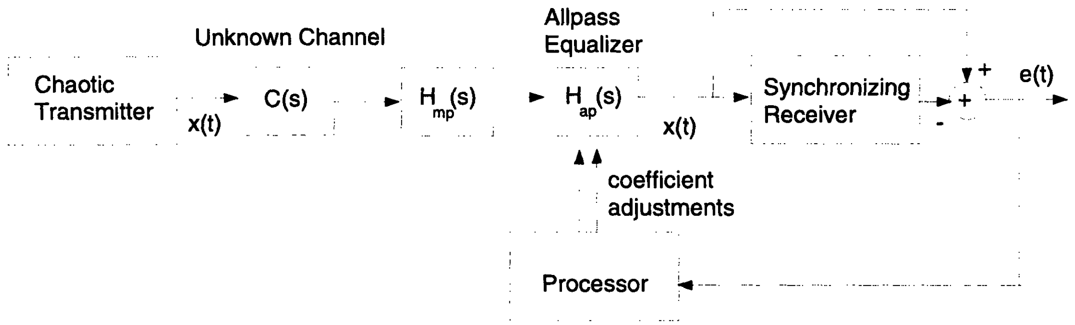

Figure 5-2: Steepest Descent Implementation for Minimum Phase/Allpass equalizer

order N with identical magnitudes. Using this conclusion, we can more intelligently initialize the equalizer with an appropriate phase.

An N^{th} order minimum phase solution is determined by the spectral division outlined in the last chapter. We can determine the synchronization error power for each of the 2^N filters with the same magnitude response. The most appropriate choice for the initial seed for the steepest descent method is the filter with the minimum error power. This approach will often ensure that the routine is initially in the deepest basin of the error power surface, as supported by results from empirical experiments.

A steepest descent of the error power surface with respect to FIR equalizer coefficients will modify both the equalizer magnitude and phase at each descent iteration. There are instances where magnitude equalization will be degraded in order to improve phase equalization. Provided a sufficient model order and data length, the minimum phase equalizer derived from the autocorrelation normal equations provides very accurate magnitude equalization, and the following section suggests a technique that will preserve the accuracy of the magnitude estimate throughout the descent of the error power surface.

5.6 Steepest Descent with Respect to Allpass Poles

Any stable, rational filter can be expressed as the cascade of a minimum phase and an allpass filter. Consider this representation of an equalizer for an arbitrary LTI channel. The minimum phase portion of the equalizer is specified very accurately, which leaves the only unknown being the appropriate allpass filter. Again the goal is to achieve minimum synchronization error, which implies the use of a steepest descent search of the error power surface. The implementation is given in Figure 5-2 which is a slight modification of Figure 5-1. There is synchronization error feedback that now modifies the parameters of an allpass filter instead of an FIR filter to achieve minimum average error power.

An allpass filter with a real-valued impulse response has poles in complex conjugate pairs. The system function of the allpass portion of the equalizer is given by:

$$H_{ap}(z) = \prod_{k=1}^{M_r} \frac{(z^{-1} - d_k^*)}{(1 - d_k z^{-1})} \prod_{k=1}^{M_c} \frac{(z^{-1} - e_k^*)(z^{-1} - e_k)}{(1 - e_k z^{-1})(1 - e_k^* z^{-1})}, \tag{5.5}$$

where the d_k are the real poles and the e_k and e_k^* are the complex poles. The number of real poles is given by M_r and the number of complex poles is given by M_c. Equation 5.5 indicates that an allpass filter of order N is specified by $M_r + M_c$ poles. There are two degrees of freedom introduced by the real and imaginary parts of each complex pole and only one degree of freedom for every real pole. Therefore the total number of degrees of freedom is $M_r + 2M_c = N$. One can imagine moving the allpass poles into all possible arrangements on the complex plane, and determining an error power for each system function. The error power is now a function of the N degrees of freedom of the poles, as opposed to the coefficients of an FIR filter.

There are two obvious implementation issues that arise with this steepest descent method. We must first recognize that in order for the equalizer to cancel channel zeros outside the unit circle with poles, the equalizer must be anti-causal to maintain stability.

The second issue is that there is no obvious initial arrangement of the poles to be made. This is because there is virtually nothing known about the phase before the steepest descent iteration is started. In this thesis we have not fully addressed the capabilities of this algorithm. It is an area for future work.

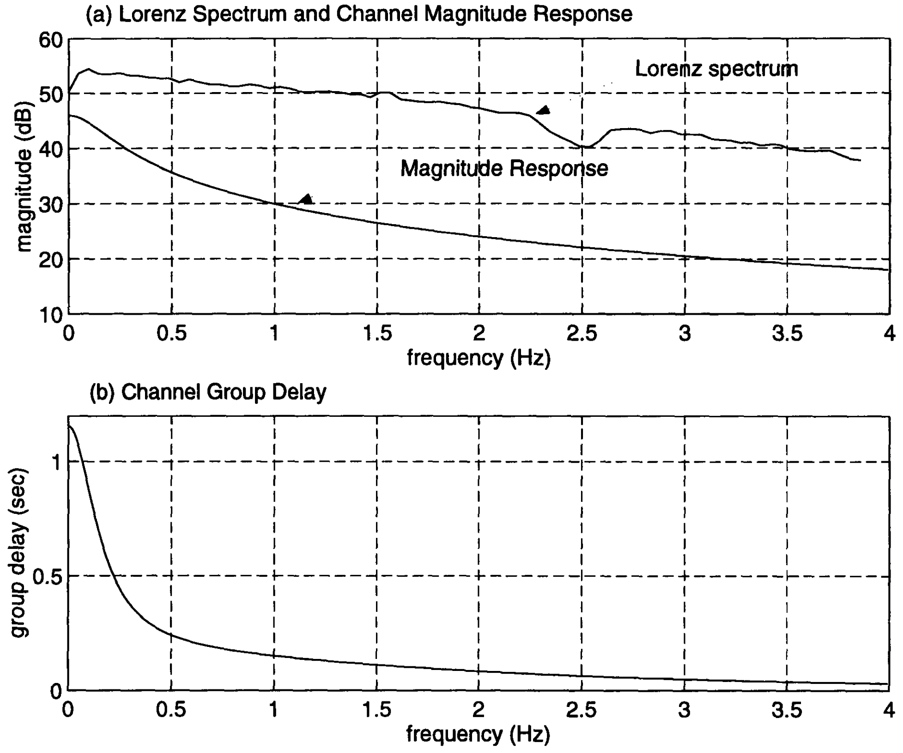

Figure 5-3: Channel Response

5.7 Numerical Experiments

In this experiment we evaluate how well the steepest descent algorithm using the FIR equalizer representation works at reducing synchronization error. We consider a non-minimum phase channel, and we equalize with both the minimum phase equalizer from the previous chapter and the equalizer determined by the steepest descent approach.

These experiments again involve the Lorenz transmitter-receiver pair, with the parameter values described in Section 1.3. The Lorenz equations were numerically integrated using a fourth order Runge-Kutte method with a fixed step size of .005. The corresponding sampling period of the received signal is $T = .005$.

Implemented in the discrete domain, the non-minimum phase channel in this experiment is selected to be the cascade of a minimum phase one-pole filter and a first order all-pass filter, where the poles of the minimum phase and allpass filters are

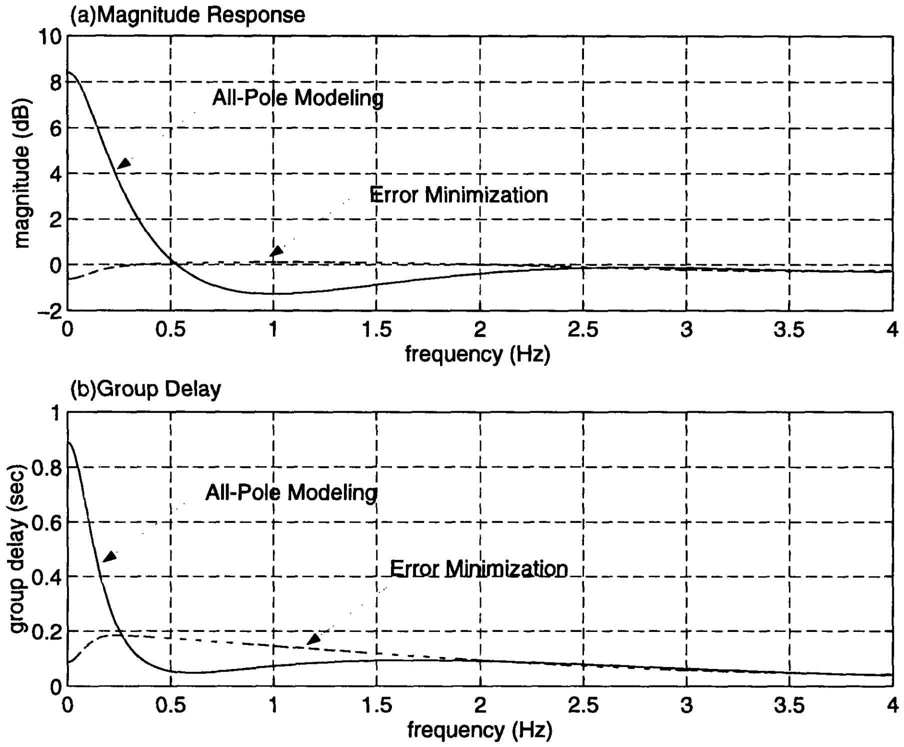

Figure 5-4: Response of channel in cascade with all-pole modeling equalizer (-) and error minimization equalizer (- -)

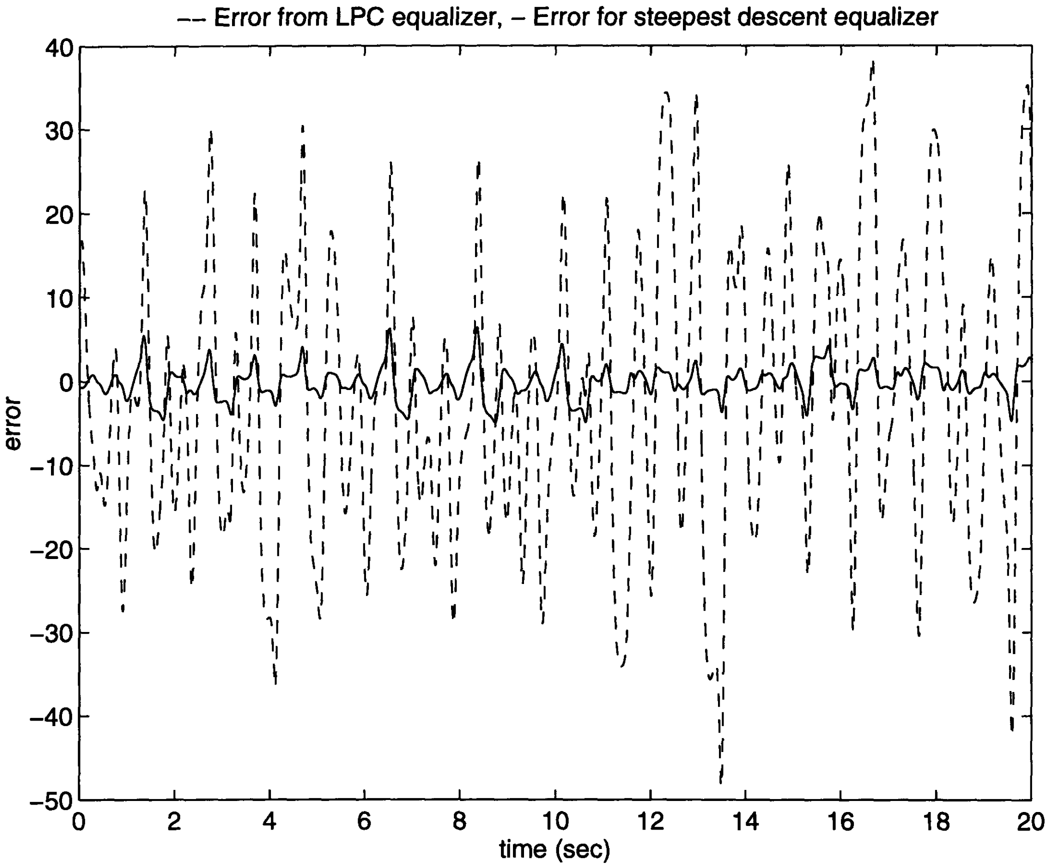

Figure 5-5: - - Error for all-pole modeling equalizer, - Error for steepest descent equalizer

at $z = .995$ and $z = .94$ respectively. The magnitude response and group delay are given in Figure 5-3.

In this experiment we determine an initial 8 point equalizer estimate by spectral division and all-pole channel modeling. The refining stage of the algorithm uses a steepest descent of the error power surface. Figure 5-4 compares the compensated channel frequency response for the all-pole modeling equalizer and the steepest descent equalizer. The desired response is unity gain and constant group delay over the band of significant input energy. Error power minimization improves significantly the all-pole modeling equalization in *both* magnitude and group delay. Figure 5-5 shows the synchronization error after equalization for both the all-pole modeling equalizer and the steepest descent equalizer. The chaos-to-error ratios are -5dB and 31dB respectively. The all-pole modeling equalizer provides virtually no improvement in synchronization error compared to no compensation, while the steepest descent equalizer provides a chaos-to-error ratio that is sufficiently low for communication. Clearly an assumption of minimum phase for all channels is unsatisfactory.

5.8 Conclusion

The challenge of general LTI equalization is very difficult, because a method of phase estimation is not obvious. Supported by empirical evidence, a steepest descent search of the error power surface with respect to FIR equalizer coefficients provides an equalizer that significantly reduces synchronization error. Warranting further study is the algorithm of Section 5.6 which attempts to more directly estimate phase by steepest descent of the error power surface with respect to allpass poles.

Chapter 6

System Identification Using Self-Synchronizing Chaotic Signals

6.1 Introduction

In addition to resolving some channel distortion issues for communication with chaotic signals, the methods uncovered in this thesis may also be valuable for system identification. Prior to this discussion, we assume we observe only the channel output and know only the dynamics of the system from which the channel input is generated. In a system identification scenario the exact channel input may also be known. Traditionally system identification is done by feeding a white noise source to a channel and calculating the magnitude and phase response by spectral division. Because now the input is known, the cross-spectrum between input and output signals may be calculated. Consider a channel $C(s)$, a stochastic input $x(t)$ and an output $y(t)$. The channel frequency response obeys the relationship:

$$C(j\omega) = \frac{P_{xy}(j\omega)}{P_{xx}(j\omega)} \tag{6.1}$$

where $P_{xy}(j\omega)$ is the cross-spectrum of the input and output and $P_{xx}(j\omega)$ is the spectral density of the input. In practice the spectra are only estimated and will not be known exactly. Because the spectral estimates are calculated by time averaged peridograms, the variance of the estimate of $C(j\omega)$ is reduced by longer observations of input and output.

For system identification an advantage of using self-synchronizing chaotic signals over stochastic signals is that the chaotic signals have properties in addition to statistics to aid in the estimation of the channel frequency response. In particular, a steepest descent of the chaotic receiver error power surface relative to FIR equalizer coefficients should improve the spectral division estimate. Clearly this method can only address an autoregressive channel model applied to the frequency response.

It is difficult to identify an error criterion for optimal system identification. For a fixed order model, the all-pole modeling method gives the autoregressive representation of a channel that has minimum mean squared magnitude error relative to the actual channel magnitude. Such an error criterion for system ID is unsatisfactory however, since it completely ignores the phase of the channel, and phase distortion is as corruptive as magnitude distortion in many applications.

This discussion leaves an open question: What is an optimal error criterion for system identification, and how might minimization of receiver synchronization error be mapped to such an error criterion? We have not definitely answered this question, but qualitative evaluation of empirical evidence suggests that there is promise for the use of self-synchronizing chaotic signals for system identification.

6.2 Numerical Experiment

There are two input sequences considered in this experiment:

1. 128 points of a Lorenz drive signal sampled at $T = .04\ sec$
2. A 128 point uniformly distributed i.i.d. noise sequence with the same variance as the Lorenz drive.

The channel is implemented digitally and is chosen to have 3 poles at $z = .995, .995e^{\pm j\omega\pi/2}$, which correspond to dc and $\pm 6Hz$ for the Lorenz signal. It must

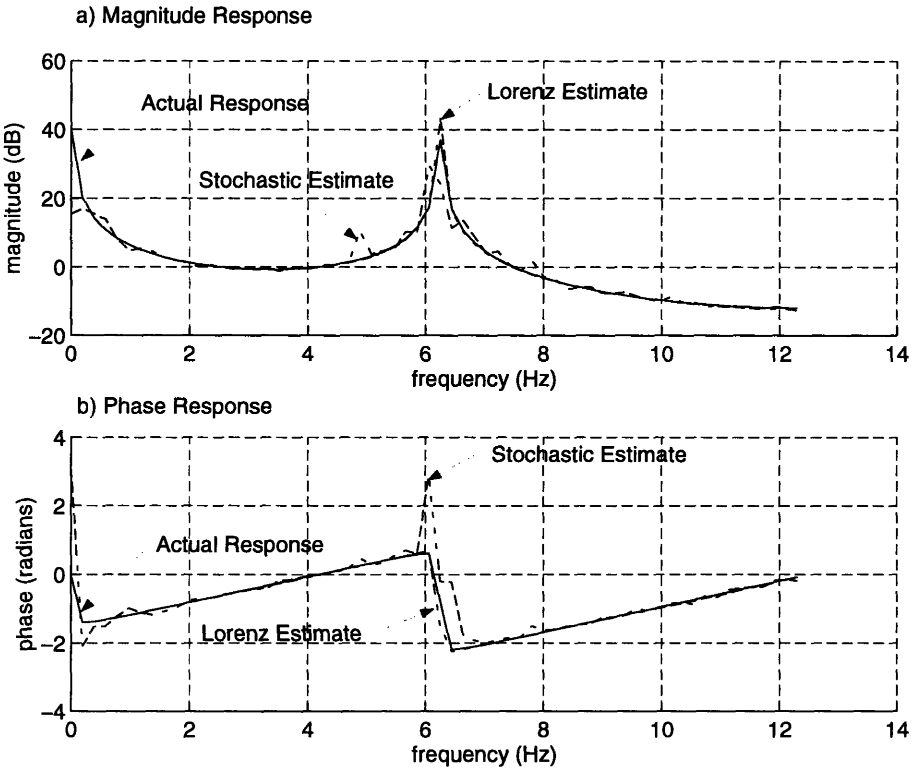

Figure 6-1: a) Channel magnitude response (-), stochastic estimate (-.), and Lorenz estimate (- -). b) Phase response

be noted that channel ID with the Lorenz signal is possible only in the band in which it has energy.

The above short data-length signals are input into the channel. The spectral density and cross-spectra are calculated by periodogram averaging, and the frequency response estimate is then determined by Equation 6.1.

The estimate from Equation 6.1 is all that can be made from the stochastic signal (Sequence 2). Figure 6-1 shows the actual frequency response and the estimates using the stochastic signal and the self-synchronizing chaotic signal. Due to the short input signal length, there is significant variance in the estimate derived from Sequence 2, especially around *dc* and $6Hz$.

The approach used with Sequence 1 was to use the spectral division frequency response estimate to derive a reasonable equalizer by inverse FFT and truncation. The resulting equalizer is used as a starting point for the gradient descent of the receiver error power surface. The intuition is that the spectral division yields a filter that lies in a basin of the error power surface, and an error minimum is easily achieved. The results in Figure 6-1 show that the experiment confirms the conjecture. Use of the Lorenz signal for this particular system identification much improves the phase and magnitude estimates over a purely stochastic signal.

We have carried out a fairly simplistic experiment, but with very positive results. If there exists a constraint on input data length for system identification, using a self-synchronizing chaotic signal may prove more fruitful than conventional stochastic methods. Self-synchronizing chaotic signals possess a great density of both *phase and magnitude* information that can be easily exploited.

Chapter 7

Summary and Contributions

This thesis was motivated by the interest in utilizing self-synchronizing chaotic signals in communications. Synchronization of the receiver to the transmitter requires that the received signal be undistorted. Any channel distortion in the form of amplitude, spectral or phase modification must be appropriately equalized. In this thesis we attempted to exploit the properties of self-synchronizing signals and systems, in particular the statistics of the signals and the self-synchronizing property of the receiver to equalize channel distortions. We approached the channel equalization problem progressively from the simplest channel model, channel gain, through to a linear time-invariant system channel model.

7.1 Channel Gain Equalization

We first considered channel gain, both constant and time-varying. It is important to consider this class of channel. For example, in a wireless communication environment, channel distortion is often in the form of gain. In particular, a fading channel is a channel whose gain is time varying. This thesis has proposed two strategies for channel gain compensation: *average power normalization* and *adaptive error minimization.* The first strategy is to normalize the average power of the received signal to the expected power of the self-synchronizing drive signal. A feature of average power normalization that is of practical interest is that its performance is not significantly degraded by time-varying gain of sufficiently small amplitude. This robustness property may prove valuable in an actual communications system operating in a fading channel environment.

The second strategy is adaptive error minimization. This method utilizes the self-synchronizing property of the receiver and the unimodalty of the error power versus gain function to attempt to achieve minimum overall error. Although much better at reducing synchronization error than average power normalization for constant channel gains, adaptive error minimization is not as robust to time-varying gains. We must conclude then, that under certain time-varying channel conditions, it is not advantageous to use adaptive error minimization after average power normalization. In some instances adaptive error minimization may actually degrade the equalization. Some engineering judgment must be used to determine whether adaptive error minimization will actually improve channel equalization.

7.2 Equalization of Minimum Phase Channels

Linear time-invariant (LTI) channel equalization was first addressed under the simplifying assumption that the channel is minimum phase. If a filter is minimum phase, its magnitude and phase are uniquely related. In light of this fact we proposed that an equalizer may be derived by first estimating the channel magnitude by spectral division; the entire equalizer frequency response is then derived by exploiting the unique Hilbert transform relationship between magnitude and phase. Successful implementation of this approach requires careful consideration of how to deal with the ill-conditioned channel magnitude estimate due to the band-limited channel input.

Experiments have shown that given prior assurance that a channel is minimum phase, equalizers can be designed to provide levels of synchronization error acceptably low for communication. The experiments in this thesis assumed no additive noise in the system, however, and additive noise may significantly affect the level of synchronization error. For instance, consider a noise source at the receiver and a channel that has significant attenuation in a certain band of frequencies. An attempt to invert the channel will magnify the noise to levels that will adversely affect synchronization. Barring such extreme situations, however, very accurate minimum phase channel inversion is possible that will yield significantly low synchronization error.

The assumption that an unknown channel is minimum phase is often not appropriate, and the described method is not well suited for non-minimum phase equalization. We have presented this strategy for minimum phase inversion, not as a problem solution, but rather as a first step toward an algorithm for the equalization of all linear time-invariant channels.

7.3 Equalization of Linear Time-Invariant Channels

In this thesis we suggested an approach for equalizing linear time-invariant channels of arbitrary magnitude and phase responses by utilizing the self-synchronization property of the receiver. We assumed that all signals are appropriately sampled and approached the issue from a discrete-time perspective. Given that the equalizer is a length N FIR filter, there exists an N dimensional synchronization error power surface, and we wish to find its minimum. We proposed that an appropriate strategy for finding the minimum error power is a steepest descent method.

It is important to initialize the steepest descent with a filter of appropriate phase. We have suggested that the most appropriate filter from which to start the steepest descent is one whose magnitude is determined from spectral division. Given an equalizer of length N, the appropriate phase of this initial filter is determined by an exhaustive search of the 2^N filters whose magnitudes are equal. The filter that yields the minimum error is the starting point for the steepest descent. Clearly a disadvantage of this method is that the number of filters to be searched grows exponentially with filter order.

Experiments have confirmed that a steepest descent of the error power surface does in fact significantly reduce synchronization error. The same experiments confirm that this reduction of synchronization error corresponds to channel inversion, i.e. the frequency response of the cascade of the channel and equalizer approaches unity magnitude and constant group delay.

The error power surface for some channels may have several local minima. The steepest descent algorithm may converge on a local minimum that provides an unsatisfactory level of synchronization error. To avoid convergence to undesirable local minima, future work may address the use of optimization algorithms that are more sophisticated than steepest descent. Such algorithms include steepest descent with momentum, Gauss-Newton methods, quasi-Newton methods, and random search methods.

Overall, the empirical evidence in this thesis regarding steepest descent of the error power surface has very positive results. If a self-synchronizing chaotic communications system were to be designed in the future, such an channel equalization scheme could be effective. Certain systems, however, may be intolerant to errors in equalization caused by convergence to a local minimum solution on the error power surface.

The above described steepest descent method adjusts both the magnitude and phase of the equalizer in search of the error power minimum. Given that spectral division yields a very accurate channel magnitude estimate, it is perhaps more logical to exclusively modify the phase of the equalizer during a descent of the error power surface. We have proposed another steepest descent approach in which the equalizer is composed of a cascade of a minimum phase filter and an all-pass filter. The minimum phase filter remains fixed throughout the gradient descent, while the poles of the all-pass filter are modified to obtain a minimum error. Future work could include a full assessment of the effectiveness and feasibility of such a scheme.

7.4 System Identification Using Self-Synchronizing Chaotic Signals

In addition to resolving some channel distortion issues for communication with chaotic signals, the methods discussed in this thesis may also be valuable for system identification. If there exists a constraint on input data length for system identification, using a self-synchronizing chaotic signal may yield better results than conventional stochastic methods. Although we were unable to quantify the performance of system identification with self-synchronizing chaotic signals, we have provided an example that qualitatively indicates its effectiveness. Based on our positive results, the use of self-synchronizing chaotic signals in system identification warrants further investigation.

Appendix A

Approximate Analysis of the Effect of Linearly Varying Channel Gain on an Average Power Estimate

In this appendix we will show that to the first order, the mean and variance of the average power estimate of a received self-synchronizing chaotic signal for a linearly varying gain channel is approximately equal to that for the constant gain channel. We will refer to the self-synchronizing drive signal as $x(t)$. The stationarity assumptions about $x(t)$ allow for us to consider the power estimate about $t = 0$ without loss of generality. We assume the estimator windows are symmetric about $t = 0$, i.e. $[-\Delta, +\Delta]$.

Throughout this discussion we will assume stationarity of the self-synchronizing drive up to fourth order statistics, and that the autocorrelation functions of $x(t)$ and $x(t)^2$ are approximately white. The whiteness assumption is valid because relative to the size of the window, the signals quickly decorrelate, and the power spectrum of self-synchronizing drive signals are flat for a considerable band of frequencies.

A.1 Case 1: Power Estimate for Constant Gain

Consider first the mean and variance of the power estimate, $P_s(t)$, for constant gain $G(t) = K$. The received signal is $s(t) = Kx(t)$. The stationarity assumptions allow for us to consider the power estimate about $t = 0$ without loss of generality. Recalling equation 3.2 the mean (μ_P) and variance (σ_P^2) of $P_s(0)$ are expressed below:

$$\begin{aligned}
\mu_P = E[P_s(t)] &= E[\frac{1}{2\Delta}\int_{-\Delta}^{\Delta} s^2(\tau)d\tau] \\
&= \frac{1}{2\Delta}\int_{-\Delta}^{\Delta} K^2 E[x^2(\tau)]d\tau \\
&= \sigma_x^2 K^2
\end{aligned}$$

$$\begin{aligned}
\sigma_P^2 &= E[P_s(t)^2] - \mu_P^2 \\
&= E[\frac{1}{(2\Delta)^2}\int_{-\Delta}^{\Delta} s^2(\tau)d\tau \int_{-\Delta}^{\Delta} s^2(\gamma)d\gamma] - \mu_P^2 \\
&= \frac{1}{(2\Delta)^2}\int_{-\Delta}^{\Delta}\int_{-\Delta}^{\Delta} K^4 E[x^2(\tau)x^2(\gamma)]d\tau d\gamma - \mu_P^2 \\
&= \frac{1}{(2\Delta)^2}\int_{-\Delta}^{\Delta}\int_{-\Delta}^{\Delta} K^4(E[x^4]\delta(\gamma-\tau) + \sigma_x^4)d\tau d\gamma - \mu_P^2 \\
&= \frac{E[x^4]}{2\Delta}K^4 + K^4\sigma_x^4 - K^4\sigma_x^4 = \frac{E[x^4]}{2\Delta}K^4
\end{aligned}$$

where σ_x^2 is the variance of the zero-mean drive signal.

A.2 Case 2: Power Estimate for Linearly Varying Gain

We next consider a linearly increasing $G(t) = G_L(t)$ about $t = 0$.

$$G_L(t) = K + \frac{\epsilon}{\Delta}(t). \tag{A.1}$$

K is the channel gain for $t = 0$ and ϵ is the maximum deviation of $G(t)$ from K in the window. We will show that for the given assumptions on $G(t)$ and a small ϵ, the average power estimator in Eq. 3.2 has approximately the same mean and variance as for a constant channel gain $G(t) = K$.

The received signal is now $s(t) = G_L(t)x(t)$. The mean of the power estimate is μ_{PL} and the variance is σ_{PL}. They are described below.

$$\begin{aligned}
\mu_{PL} &= E[P_s(t)] \\
&= E[\frac{1}{2\Delta}\int_{-\Delta}^{\Delta} s^2(\tau)d\tau] \\
&= \frac{1}{2\Delta}\int_{-\Delta}^{\Delta}[K^2 + 2K\frac{\epsilon}{\Delta}\tau + (\frac{\epsilon}{\Delta})^2\tau^2]E[x^2(\tau)]d\tau \\
&= \sigma_x^2(K^2 + \epsilon^2/3)
\end{aligned}$$

$$\begin{aligned}
\sigma_{PL} &= E[P_s(t)^2] - \mu_{PL}^2 \\
&= E[\frac{1}{(2\Delta)^2}\int_{-\Delta}^{\Delta} s_L^2(\tau)d\tau \int_{-\Delta}^{\Delta} s^2(\gamma)d\gamma] - \mu_{PL}^2 \\
&= \frac{1}{(2\Delta)^2}\int_{-\Delta}^{\Delta}\int_{-\Delta}^{\Delta} G_L^2(\tau)G_L^2(\gamma)E[x^2(\tau)x^2(\gamma)]d\tau d\gamma - \mu_{PL}^2 \\
&= \frac{1}{(2\Delta)^2}\int_{-\Delta}^{\Delta}\int_{-\Delta}^{\Delta} G_L^2(\tau)G_L^2(\gamma)(E[x^4]\delta(\gamma-\tau) + \sigma_x^4)d\tau d\gamma - \mu_{PL}^2 \\
&= \frac{1}{(2\Delta)^2}\int_{-\Delta}^{\Delta}[K^4 + 4K^3\frac{\epsilon}{\Delta}\tau + (2K^2 + 4K)\frac{\epsilon}{\Delta}\tau^2 \\
&\quad +4K(\frac{\epsilon}{\Delta})^3\tau^3 + (\frac{\epsilon}{\Delta})^4\tau^4]E[x^4]d\tau \\
&= \frac{E[x^4]}{2\Delta}(K^4 + \frac{\epsilon^2}{3}(2K^2 + 4K) + \frac{\epsilon^4}{5})
\end{aligned}$$

To the first order (in ϵ), the mean and variance of the power estimate for the linearly varying channel gain are approximately equal to those for the constant gain case. So for strictly increasing or strictly decreasing channel gains of small slope, the average power normalization should reduce synchronization error nearly as effectively as for constant gain. Empirical studies have concurred with these conclusions.

Bibliography

[1] Strogatz S. H. *Non-Linear Dynamics and Chaos.* Addison-Wesley Publishing. Reading, MA. 1994.

[2] Cuomo, K.M., Oppenheim, A.V., Kevin M. Cuomo, Isabelle S.H. "Spread Spectrum Modulation and Signal Masking Using Synchronized Chaotic Systems." Technical Report 570, MIT Research Laboratory of Electronics, February 1992.

[3] Oppenheim, A.V., Wornell, G.W., Isabelle, S.H., and Cuomo, K.M., "Signal Processing in the Context of Chaotic Signals," in *Proc. of 1992 IEEE ICASSP* **IV**, pp. 117-120, 1992.

[4] Cuomo, K.M., Oppenheim, A.V., and Strogatz, S.H., "Robustness and signal recovery in a synchronized chaotic system," *Int. J. Bif. Chaos* **3**(6), pp. 1629-1638, 1993.

[5] Cuomo, K.M. *Analysis and Synthesis of Self-Synchronizing Chaotic Systems.* PhD Thesis, EECS, Massachusetts Institute of Technology, Cambridge, MA, February 1994.

[6] Pecora, L.M., and Carroll, T.L., "Synchronization in chaotic systems," *Phys. Rev. Lett.* **64**(8), pp. 821-823, 1990.

[7] K. M. Cuomo, "Synthesizing self-synchronizing chaotic systems", *Int. J. of Bifurcation and Chaos*, **3**, pp.1327-1337, (1993).

[8] Cuomo, K.M., Oppenheim, A.V., and Strogatz, S.H., "Synchronization of Lorenz-based chaotic circuits with applications to communications," *IEEE Trans. Circuits and Syst.* **40**(10), pp. 626-633, 1993.

[9] Eckmann, J.P., and D. Ruelle. "Ergodic Theory of Chaos and Strange Attractors." *Review of Modern Physics*, 57(3):627-656, July 1985.

[10] Jackson L. B. *Digital Filters and Signal Processing.* Kluwer Academic Publishers. Boston. 1986.

[11] Li H., Farhat, N.H., and Shen Y. " A new iterative algorithm for extrapolation of data available in multiple restricted regions with application to radar imaging." *IEEE Transactions on Antennas and Propagation* **AP-35**(1), pp. 581-8, 1987.

[12] Cuomo, K.M., Oppenheim, A.V., and Barron, R.J., " Channel Equalization for Self-Synchronizing Chaotic Systems," *Proc. 1996 IEEE ICASSP.* This paper has not yet been published.

[13] Barda, A., and Laufer, S., "Multiple user receivers for CDMA networks based on chaotic signals," submitted to *IEEE Journal on Selected Areas in Communications*, special issue on *Wireless Local Communications*, 1995.

[14] Cuomo, K.M., and Oppenheim, A.V., "Circuit implementation of synchronized chaos with applications to communications," *Phys. Rev. Lett.* **71**(1), pp. 65-68, 1993.

[15] Cuomo, K.M., and Oppenheim, A.V., "Synchronized chaotic circuits and systems for communications," *Technical Report 575*, MIT Research Laboratory of Electronics, 1992.

[16] Halle, K.S., Wu, C.W., Itoh, M., and Chua, L.O., "Spread spectrum communication through modulation of chaos," *Int. J. Bif. Chaos* **3**(2), pp. 469-477, 1993.

[17] Kocarev, Lj., Halle, K.S., Eckert, K., and Chua, L.O., "Experimental demonstration of secure communications via chaotic synchronization," *Int. J. Bif. Chaos* **2**(3), pp. 709-713, 1992.

[18] Parlitz, U., Chua, L.O., Kocarev, Lj., Halle, K.S., and Shang, A., "Transmission of digital signals by chaotic synchronization," *Int. J. Bif. Chaos* **2**(4), pp. 973-977, 1992.

[19] Carroll, T.L., and Pecora, L.M., "Synchronizing chaotic circuits," *IEEE Transactions on Circuits and Systems* **38**(4), pp. 453-456, April 1991.

[20] Oppenheim, A.V., Cuomo, K.M., Barron, R.J., and Freedman, A.E., "Channel Equalization for Communication with Chaotic Signals," *Proc. The 3rd Technical Conference on Nonlinear Dynamics (CHAOS) and Full Spectrum Processing*, July 1995.

[21] Cuomo, K.M., and Oppenheim, A.V., " Chaotic Signals and Systems for Communications," *Proc. 1993 IEEE ICASSP* **3**, pp. 137-140, 1993.